Stability of the compressible laminar boundary layer

By LESTER LEES AND ELI RESHOTKO†

Guggenheim Aeronautical Laboratory, California Institute of Technology, Pasadena, California

(Received 21 July 1961 and in revised form 3 November 1961)

In previous theoretical treatments of the stability of the compressible laminar boundary layer, the effect of the temperature fluctuations on the viscous (rapidly varying) disturbances is accounted for incompletely. A thorough re-examination of this problem shows that temperature fluctuations have a profound influence on both the inviscid (slowly varying) and viscous disturbances above a Mach number of about 2·0. The present analysis includes the effect of temperature fluctuations on the viscosity and thermal conductivity and also introduces the viscous dissipation term that was dropped in the earlier theoretical treatments.

Some important results of the present study are: (1) the rate of conversion of energy from the mean flow to the disturbance flow through the action of viscosity in the vicinity of the wall increases with Mach number; (2) instead of being nearly constant across the boundary layer, the amplitude of inviscid pressure fluctuations for Mach numbers greater than 3 decreases markedly with distance outward from the plate surface. This behaviour means that the jump in magnitude of the Reynolds stress in the neighbourhood of the critical layer is greatly reduced; (3) at Mach numbers less than about 2, dissipation effects are minor, but they become extremely important at higher Mach numbers, since for neutral disturbances they must compensate for the generally destabilizing effects of items (1) and (2); (4) the minimum critical Reynolds number for an insulated flat plate boundary layer decreases with increasing Mach number in the range $0 \leqslant M_e \leqslant 3$.‡ Since the wave-number varies like $1/M_e^2$ when $M_e \gg 1$, the minimum critical Reynolds number is likely to increase sharply at hypersonic speeds.

Numerical examples illustrating the effects of compressibility, including neutral stability characteristics, are obtained and are compared with the experimental results of Laufer & Vrebalovich (1960) at Mach 2·2, and of Demetriades (1960) at Mach 5·8.

1. Introduction

The stability of a compressible laminar boundary layer to infinitesimal disturbances was first analysed by Lees & Lin (1946) and Lees (1947). Their study was in the form of an extension to compressible flow of the principles and techniques already formulated for the study of the stability of incompressible laminar boundary layers. Lees & Lin uncovered some of the important changes, both

† Now at Lewis Research Center—NASA, Cleveland, Ohio.

‡ A full list of symbols is given at the end of this paper.

physical and mathematical, that are incurred by considering compressibility in the stability analysis. More recently there have been additional analyses (Cheng 1953; Dunn 1953; Dunn & Lin 1955) and also two experiments (Laufer & Vrebalovich 1958, 1960; Demetriades 1958, 1960), which have clarified the stability picture for subsonic and slightly supersonic boundary layers, but have hardly been successful in the case of supersonic and hypersonic laminar boundary layers. The purpose of the present study is to probe into the effects of compressibility on the various physical processes associated with the stability phenomenon.

The present study considers only 'subsonic' disturbances, that is, disturbances whose propagation velocity is subsonic with respect to the free-stream velocity $[(1-1/M_e) < c < 1]$. (See end of paper for definition of symbols.) Such disturbances have amplitudes that decay exponentially in the free stream. A disturbance that propagates supersonically with respect to the free stream would be expected to have a non-vanishing amplitude far from the wall. It may be noted that, in the recent experiment at Mach number 2·2 by Laufer & Vrebalovich (1958, 1960), supersonic disturbances were not detected and reasonable agreement was obtained with the theory of infinitesimal subsonic disturbances.

For subsonic and slightly supersonic flows, Lees & Lin (1946) concluded that the stability characteristics of a given boundary-layer profile are unaffected by the boundary conditions on temperature fluctuations. More specifically, the characteristics are determined by satisfying only the velocity-fluctuation boundary conditions. Dunn & Lin (1955) found that this conclusion is not valid for moderately high supersonic Mach numbers, and they gave some discussion of the thermal boundary condition. However, they did not present any calculations that include consideration of the energy equation and thermal boundary conditions.

The analyses of Lees & Lin and Dunn & Lin are first-order asymptotic approximations valid when a parameter (αRe), the product of wave-number and Reynolds number, is very large. Among the terms that do not enter into this first asymptotic approximation are terms involving dissipation and terms involving fluctuating viscosity and fluctuating thermal conductivity. Cheng (1953) points out that terms involving vertical velocity enter into the second approximation. It will be pointed out later that a dissipation term and some terms involving fluctuating transport properties also enter in the second approximation. Since some of these terms increase in magnitude with increase in Mach number, it is necessary to include them at high Mach number.

In the past, approximate methods have been used to solve the asymptotic equations. These methods were valid only for small values of the wave-number and for propagation velocities that are not very close to the free-stream velocity. For supersonic and hypersonic Mach numbers, larger values of wave-number and propagation velocities approaching free-stream velocity are encountered and more exact numerical methods will be considered.

The present study then considers the stability of two-dimensional compressible laminar boundary layers to two-dimensional subsonic disturbances. Only the simplest model of a compressible gas is considered—namely, one with constant specific heats, constant Prandtl number, and viscosity a function of temperature

alone. The analysis considers both insulated and uninsulated surfaces; however, the numerical examples will be for insulated surfaces only, and comparison will be made with the experimental findings of Laufer & Vrebalovich (1958, 1960) and of Demetriades (1958, 1960).

Lastly, in § 5 the effects of compressibility on the physical concepts of the boundary-layer stability phenomenon are discussed with the aid of some approximate calculations. Those readers having some familiarity with the stability problem at low speeds may want to read this section first.

2. Formulation of problem

2.1. *Differential equations for infinitesimal disturbances*

Quantities of the total flow such as velocity and temperature are considered to be composed of a mean or steady component that depends only on the space coordinates, and a space-and-time-dependent fluctuating component of infinitesimal magnitude; thus

$$Q(x, y, t) = \bar{Q}(x, y) + Q'(x, y, t). \tag{1}$$

Because the fluctuation amplitudes are very small compared to the mean flow quantities, products and squares of fluctuation quantities are neglected. The resulting disturbance equations are then linear partial differential equations in the variables x, y and t.

If the mean flow $\bar{Q}$ is a time-independent parallel flow (no mean normal velocities), and if in addition $\bar{Q}$ is independent of x (fully developed flow), then the coefficients of the linear partial differential disturbance equations are independent of both x and t and a disturbance of the form

$$Q' = q(y)\, e^{i\alpha(x-ct)} \tag{2}$$

will reduce the disturbance equations to ordinary differential equations in y alone. The disturbance amplitude $q(y)$ and the propagation velocity c in equation (2) are taken to be complex. Disturbances are amplified, neutral, or damped according to whether $c_i > 0$, $c_i = 0$, or $c_i < 0$, respectively. The real part c_r is the dimensionless wave speed.†

Lees & Lin (1946) proposed the use of the parallel-flow disturbance equations for 'nearly-parallel' boundary-layer flows. Therefore, they omitted terms of the following types from the complete disturbance equations: (1) terms involving mean normal velocity $\bar{v}^*$ (the ratio $\bar{v}^*/\bar{u}^*$ is of order M_e^2/Re_θ or M_e^4/Re_δ and is assumed to be small for high Reynolds numbers); (2) longitudinal derivatives of mean flow quantities as compared with their normal derivatives; and (3) longitudinal derivatives of disturbance amplitudes. For a disturbance of the form (2),

† Equation (2) is not the only disturbance form possible for parallel flows. It is of some interest in fact to investigate amplified and damped disturbances of the form

$$Q' = q(y)\, e^{\beta x}\, e^{i\alpha(x-ct)},$$

where α, β, and c are all real. Here $\beta = (\overline{Q'^2})^{-\frac{1}{2}}\, \partial\{(\overline{Q'^2})\}^{\frac{1}{2}}/\partial x$ is the amplification coefficient. For neutral disturbances, $\beta = 0$, and the analysis is the same as that for $c_i = 0$ in equation (2).

the dimensionless equations for infinitesimal disturbances in a nearly parallel mean flow are as follows (Lees & Lin 1946):

Continuity: $$\phi' + if - (T'/T)\,\phi + i(w-c)\,(\pi - \theta/T) = 0. \tag{3}$$

Momentum:

$$\alpha\rho[i(w-c)f + w'\phi] = -(i\alpha\pi/\gamma M_e^2) + (\mu/Re)\,[f'' + \alpha^2(i\phi' - 2f)] + (2/3Re)\,(\mu_2 - \mu)\,\alpha^2(i\phi' - f) + (1/Re)\,[mw'' + m'w' + \mu'(f' + i\alpha^2\phi)], \tag{4}$$

$$\alpha^2\rho[i(w-c)\,\phi] = -(\pi'/\gamma M_e^2) + (\mu\alpha/Re)\,(2\phi'' + if' - \alpha^2\phi) + (2/3Re)\,\alpha(\mu_2 - \mu)\,(\phi'' + if') + (\alpha/Re)\,[imw' + 2\mu'\phi' + \tfrac{2}{3}(\mu_2' - \mu')\,(\phi' + if)]. \tag{5}$$

Energy:

$$\alpha\rho[i(w-c)\,\theta + T'\phi] = i\alpha(w-c)\,(1-\gamma^{-1})\,\pi + [(\gamma-1)M_e^2/Re] \times [mw'^2 + 2\mu w'(f' + i\alpha^2\phi)] + (1/\sigma Re)\,[\mu(\theta'' - \alpha^2\theta) + (mT')' + \mu'\theta']. \tag{6}$$

The density fluctuations have been eliminated in the preceding equations through the equation of state: $r/\rho = \pi - (\theta/T)$. The energy equation (6) differs slightly from that of Lees & Lin in that it is derived from the enthalpy equation rather than from the internal-energy equation. The fluctuating viscosity can be related to the temperature fluctuation through $m = \theta(d\mu/dT)$, while the normal gradient of mean viscosity can be expressed as $\mu' = T'(d\mu/dT)$.

2.2. *Boundary conditions*

For flows over non-porous surfaces, the longitudinal and normal velocity components of the total unsteady flow must vanish at the surface. Since the mean flow already satisfies these conditions, the disturbance-velocity amplitudes must also vanish at the surface. Thus,

$$f_w = 0, \quad \phi_w = 0. \tag{7, 8}$$

The thermal boundary condition for the total unsteady flow is that the instantaneous temperature and heat transfer must be continuous across the solid-gas interface. However, most surface materials are highly conductive compared to gases and so would immediately damp any temperature fluctuations at the frequencies of interest for laminar stability. Therefore, we take†

$$\theta_w = 0. \tag{9}$$

Since only subsonic disturbances are here considered (see § 1), all disturbance amplitudes vanish far from the wall, i.e.,

$$q(y) \to 0 \quad \text{as} \quad y \to \infty. \tag{10}$$

3. Solution of differential equations

As discussed in Lees & Lin (1946), the disturbance equations (3) to (6) are regular everywhere except in the limit $y \to \infty$; and the solutions of these equations are analytic functions of α, c, and Re for all finite values of these parameters. In

† The formulation of the stability problem for the more general thermal boundary condition $a\theta_w' + b\theta_w = 0$ is given in Appendix F of Reshotko (1960).

principle, solutions could be constructed as convergent series expansions around one or more regular points, and these series could be properly joined to exponentially decaying functions as $y \to \infty$. However, the quantity $(\alpha Re)^{-1}$ appears in the disturbance equations as a parameter multiplying the highest-order derivatives, and it is attractive to consider asymptotic expansions valid for $(\alpha Re) \gg 1$.

In particular, we inquire as to the significance of the solutions obtained in the limit of $(\alpha Re) \to \infty$. In general, these 'inviscid' solutions are certainly incapable of satisfying the boundary conditions $f_w = 0$ and $\theta_w = 0$ at the surface. Thus, for any finite value of (αRe), viscous solutions that take on the values $-(f_w)_{\text{inv}}$ and $(-\theta_w)_{\text{inv}}$ at the surface must always be added (see figure 1), and the situation locally has some of the characteristics of the oscillating plate problem. Since the parameter $(\alpha Re)^{-\frac{1}{2}}$ measures the relative diffusion distance for vorticity during

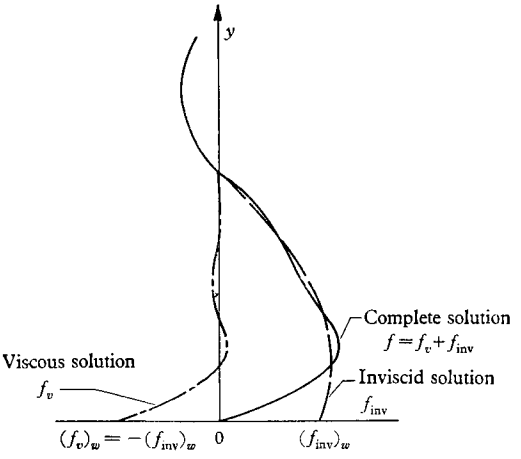

FIGURE 1. Schematic representation of viscous and inviscid solutions for f near surface. (A similar sketch could be drawn for θ.)

one period [or $(\alpha Re\sigma)^{-\frac{1}{2}}$ measures the corresponding diffusion distance for heat energy], this 'inner boundary layer' is thin when $(\alpha Re) \gg 1$. Thus we are led to adopt Prandtl's (Prandtl 1935) division of the disturbances into slowly varying functions that are largely inviscid across the entire flow, and 'viscous' rapidly varying functions near the surface. Because of the steep slope of the viscous solutions (figure 1), it is clear that the effect of viscous dissipation at high Mach numbers cannot be neglected *a priori*.

Of course, the value of αRe is not arbitrary; for a neutral disturbance (for example) it is uniquely determined by the local velocity-temperature profile and the local Mach number. At present there is no way of determining in advance whether the quantity αRe is always 'sufficiently large' for a neutral disturbance at high Mach numbers. Therefore, we shall proceed provisionally with Prandtl's suggestion, just as previous investigators have done for low-speed flow or moderate supersonic Mach numbers. However, this splitting of the solutions must be re-examined *a posteriori* to determine the conditions under which it is in fact justified and, conversely, the conditions under which we must return to the more complete disturbance equations (3) to (6).

3.1. *Inviscid solution*

Following Rayleigh, Heisenberg, and Lin, a solution to the disturbance equations of the form

$$q(y) = q_0(y) + (1/\alpha Re)\, q_1(y) + \ldots \text{ is sought.}$$

The resulting equations for the zeroth approximation (q_0) representing

$$\lim_{\alpha Re \to \infty} q(y)$$

for fixed y are called the inviscid equations, since they are identical with the equations obtained by ignoring viscosity and conductivity altogether. The inviscid equations are:

Continuity:
$$\phi' + if - (T'/T)\,\phi + i(w-c)\,[\pi - (\theta/T)] = 0. \tag{11}$$

Momentum:
$$i\rho(w-c)f + \rho w'\phi = -i\pi/\gamma M_e^2, \tag{12}$$

$$i\alpha^2\rho(w-c)\,\phi = -\pi'/\gamma M_e^2. \tag{13}$$

Energy:
$$i\rho(w-c)\,\theta + \rho T'\phi = i(w-c)\,(1-\gamma^{-1})\,\pi. \tag{14}$$

The subscript zero is omitted since the q_0 functions are the only ones that will be obtained in this manner.

In the present analysis, following a suggestion of Lighthill (1950) and some work on panel flutter by Miles (1959), the inviscid equation will be written in terms of the pressure fluctuation amplitude π. The boundary condition that the inviscid solution must always satisfy is that the normal velocity fluctuation vanish in the outer inviscid flow. If viscosity and conductivity are ignored ($\alpha Re \to \infty$), the inviscid normal-velocity-fluctuation amplitude must also vanish at the wall; therefore, for $\alpha Re \to \infty$, $\pi'(0) = 0$ by equation (13). However, for αRe large but finite, $\phi_{\text{inv}}(0) = -\phi_v(0) \neq 0$, and thus $\pi'_{\text{inv}}(0) \neq 0$.

The inviscid equation and boundary conditions are

$$\pi'' = \left(\frac{2w'}{w-c} - \frac{T'}{T}\right)\pi' + \alpha^2\left(1 - \frac{M_e^2(w-c)^2}{T}\right)\pi, \tag{15}$$

$$\pi'(0) = 0 \quad (\text{for } \alpha Re \to \infty \text{ only}), \tag{16}$$

$$\pi(\infty) \to 0. \tag{17}$$

By means of the standard transformation

$$G = \pi'/\alpha^2\pi, \tag{18}$$

equation (15) can be converted into the following first-order non-linear equation of the Riccati type

$$G' = \left(1 - \frac{M_e^2(w-c)^2}{T}\right) + \left(\frac{2w'}{w-c} - \frac{T'}{T}\right) G - \alpha^2 G^2. \tag{19}$$

The outer boundary condition on G is obtained by considering equation (15) for large y

$$\pi'' - \alpha^2[1 - M_e^2(1-c)^2]\,\pi = 0, \tag{20}$$

whose solutions are

$$\pi \sim \exp\left[\pm\{1 - M_e^2(1-c)^2\}^{\frac{1}{2}}\, y\right]. \tag{21}$$

Since $\pi(\infty) \to 0$, the negative exponent is chosen in equation (21), and the boundary conditions on G are

$$G(0) = 0 \quad (\text{for} \quad \alpha Re \to \infty \text{ only}), \quad G(\infty) = -\{1 - M_e^2(1-c)^2\}^{\frac{1}{2}}/\alpha. \qquad (22a, b)$$

It is instructive at this point to transform the inviscid equation by introducing a Dorodnitsyn–Howarth independent variable. In this form, the boundary-layer thickness is normalized.

For
$$\tilde{\eta} = \int dy/T \qquad (23)$$

and
$$\tilde{G} = \frac{1}{\alpha^2 T^2 \pi} \frac{d\pi}{d\tilde{\eta}}, \qquad (24)$$

the inviscid equation (19) becomes

$$\frac{d\tilde{G}}{d\tilde{\eta}} = \left(1 - \frac{M_e^2(w-c)^2}{T}\right) + \left(\frac{2\,dw/d\tilde{\eta}}{w-c} - \frac{2dT/d\tilde{\eta}}{T}\right)\tilde{G} - (\alpha T_{\text{ref}})^2 \left(\frac{T}{T_{\text{ref}}}\right)^2 \tilde{G}^2, \qquad (25)$$

where T_{ref} is some representative boundary-layer temperature of order 1 for low-speed flows but of order M_e^2 for high-speed flows.

Following Heisenberg, it has been customary in the past to solve the inviscid equation in the form of a convergent series in powers of α^2. Equation (25) suggests that the proper expansion parameter for the compressible inviscid solutions is $(\alpha T_{\text{ref}})^2$ or $(\alpha M_e^2)^2$ rather than α^2. At high Mach number, even for small α, the quantity (αT_{ref}) may not be small, so that the complete equation (25) must be considered.

Of course if the non-linear term in equation (19), $\alpha^2 G^2$, is suppressed, we obtain immediately the solution corresponding to the zeroth-order inviscid solution of Lees & Lin (1946), namely

$$G_r(y) = \frac{(w-c)^2}{T} \int_{y_c}^{y} \frac{T - M_e^2(w-c)^2}{(w-c)^2} dy, \quad G_i(y) = \begin{cases} \dfrac{A\pi T_c}{w_c'^2} \dfrac{(w-c)^2}{T} & \text{for} \quad y < y_c, \\ 0 & \text{for} \quad y > y_c, \end{cases}$$

where
$$A \equiv \frac{w_c''}{w_c'} - \frac{T_c'}{T_c}.$$

Equation (19) is a complex equation and for purposes of solution should be divided into real and imaginary parts. Also, there is a regular singularity of equation (19) at the point where $w = c$. This point is often called the 'critical point'. The solution in the neighbourhood of this singular point is obtained by series expansion (method of Frobenius), the details of which are given in Reshotko (1960). For a neutral disturbance ($c_i = 0$),† the resulting behaviour of G about the critical point is

$$G_r = -(y-y_c) - A(y-y_c)^2 \ln|y-y_c| + (\text{const.})(y-y_c)^2 - A^2(y-y_c)^3 \ln|y-y_c| + [A(\text{const.}) - (2B - 2A^2 + M_e^2 w_c'^2/T_c + \alpha^2)](y-y_c)^3 + \ldots. \qquad (26)$$

For $(y-y_c) > 0$,
$$G_i = 0, \qquad (27a)$$

and for $(y-y_c) < 0$,
$$G_i = A\pi(y-y_c)^2[1 + A(y-y_c) + \ldots]. \ddagger \qquad (27b)$$

† The developments for amplified and damped oscillations ($c_i \neq 0$) are very similar and are given in Appendix B of Reshotko (1960).

‡ The π appearing without subscript in equation (27*b*) is 3·14159....

Here
$$A \equiv \left(\frac{w_c''}{w_c'} - \frac{T_c'}{T_c}\right) = \frac{T_c}{w_c'}\left[\frac{d}{dy}\left(\frac{w'}{T}\right)\right]_c, \tag{28}$$

and
$$B \equiv \left(\frac{w_c''^2}{4w'^2} + \frac{w_c'''}{3w'} - \frac{T_c''}{2T_c}\right) - A\frac{T_c'}{T_c}. \tag{29}$$

It is instructive at this point to examine the nature of the inviscid equation graphically. As an example, the case of the neutral inviscid oscillation ($\alpha Re \to \infty$) is chosen. For such an oscillation, the boundary condition at the wall is that

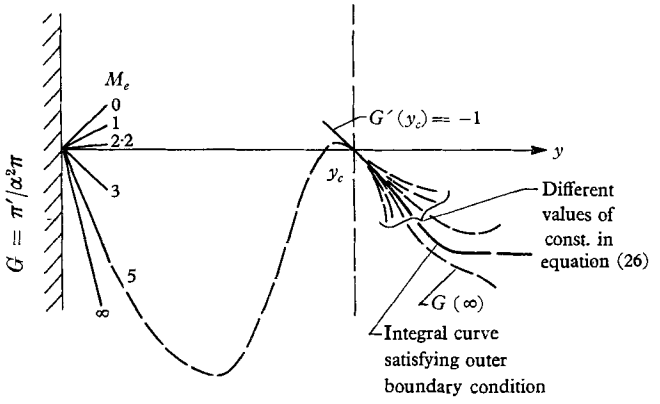

FIGURE 2. Inviscid solution for neutral inviscid disturbance ($A = 0$, $c = c_s$). $G'(0) = 1 - M_e^2 c_s^2/T_w$; $G(\infty) = -\{1 - M_e^2(1 - c_s)\}^{\frac{1}{2}}/\alpha$.

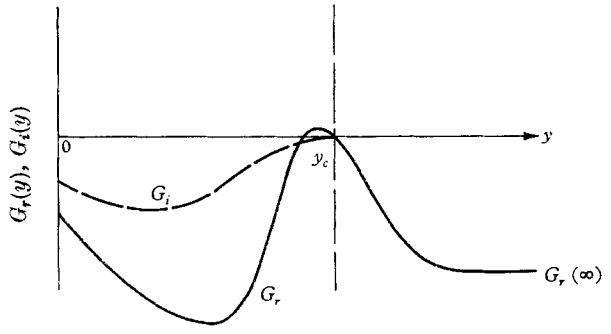

FIGURE 3. Inviscid solution for general disturbance ($A \neq 0$, $c \neq c_s$).

$G_r(0) = G_i(0) = 0$. From the imaginary part of equation (19), it is seen immediately that if G_i is zero at the wall, then G_i must be zero everywhere. Thus, from equation (27*b*), a necessary condition for a neutral inviscid oscillation is that $A \equiv 0$. Lees & Lin (1946) by a mathematical proof show that this condition is both necessary and sufficient. The value of the propagation velocity for which the condition $A = 0$ is satisfied is denoted by c_s. We are thus concerned with constructing the solution to equation (19) for $G = G_r$ with the boundary conditions

$$G(0) = 0, \quad G(\infty) = -\{1 - M_e^2(1 - c_s)^2\}^{\frac{1}{2}}/\alpha.$$

The curves in figures 2 and 3 are for insulated flat-plate boundary layers with $\gamma = 1{\cdot}4$.

Consider first the region about the critical point where the leading terms of the solution (26) are $G = -(y-y_c) + \text{const.}\,(y-y_c)^2 + \ldots$.

The slope of G at the critical point is always -1. However, the curvature at this point is an undetermined constant. For a given α only one value of this constant will yield an integral curve that satisfies the outer boundary condition (figure 2). Once this value of the constant is determined for a given α, the integration can proceed inward from the critical layer toward the wall. For $c = c_s$, the value of α for which the wall boundary condition $G(0) = 0$ is satisfied will be denoted by α_s. The integral curve for α_s approaches the wall boundary condition from above or below according to whether $G'(0) = 1-(M_e^2 c_s^2/T_w)$ is positive or negative, respectively. Some representative slopes near the wall are shown in figure 2. For $M_e = 0$, the slope at the wall is $+1$; for infinite Mach number, the slope would be -4 for Prandtl number 1. The slope $G'(0)$ is zero for a Mach number slightly above 2·2. Since $\pi/\pi_w = \exp\left[\int_0^y \alpha_s^2 G\,dy\right]$, positive areas under the G curve represent increases in pressure fluctuation amplitude relative to the wall value, while negative areas represent decreases.

The non-linear term in equation (19) is important only when G is very large. However, it is always important near the outer boundary, since the outer boundary condition is determined by a balance of the $[1-M_e^2(w-c)^2/T]$ and $[-\alpha^2 G^2]$ terms of equation (19).

The uniqueness of α_s has been conclusively demonstrated by Lees & Lin (1946) when the boundary layer is entirely subsonic relative to the disturbance. No such proof is yet available when the wall is supersonic relative to the disturbance.

For a neutral disturbance with αRe finite, the quantity A generally takes on a non-zero value ($A \lesseqgtr 0$ for $c \lesseqgtr c_s$), and G takes on an imaginary part. Also, the constant in equation (26) is no longer the curvature but only a parameter, since the curvature at the critical point is logarithmically singular for $A \neq 0$. The character of the integral curves is shown in figure 3. The curve for G is not very different from that for $A = 0$, except that $G_r(0) \neq 0$. The imaginary part G_i is always of the same sign as A and also has a non-zero wall value. These non-zero values lead to $(\phi_{\text{inv}})_w \neq 0$, $(f_{\text{inv}})_w \neq 0$, and $(\theta_{\text{inv}})_w \neq 0$, and the action of viscosity is required to cancel these inviscid contributions and satisfy the wall boundary conditions.

Once the distribution of $G(y)$ across the profile is obtained the distribution of the inviscid disturbance amplitudes are calculated as follows:

$$\pi = \exp\left(\int \alpha^2 G\,dy\right) = \exp\left(\int_{y_c}^{y} \alpha^2 G_r\,dy\right)\left\{\cos\left(\int_{y_c}^{y} \alpha^2 G_i\,dy\right) + i\sin\left(\int_{y_c}^{y} \alpha^2 G_i\,dy\right)\right\}. \tag{30}$$

This integration is carried out starting from the critical layer, since the imaginary parts of π and G_i have zero value outward from the critical layer. The real and imaginary parts of π are

$$\pi_r = \exp\left(\int_{y_c}^{y} \alpha^2 G_r\,dy\right)\cos\left(\int_{y_c}^{y} \alpha^2 G_i\,dy\right) \tag{31a}$$

and

$$\pi_i = \exp\left(\int_{y_c}^{y} \alpha^2 G_r\,dy\right)\sin\left(\int_{y_c}^{y} \alpha^2 G_i\,dy\right). \tag{31b}$$

By equation (30), the pressure fluctuation amplitudes are referred to their value at the critical layer; that is $\pi_c = \pi_{r_c} = 1$ is the reference pressure fluctuation amplitude. From the inviscid equations (11) to (14), the other fluctuation amplitudes can be related to the pressure fluctuation amplitude. Following Dunn & Lin (1955), the inviscid functions are denoted by the capital letters Φ, F, and Θ, where

$$\Phi = i\frac{T\pi'}{\gamma M_e^2\alpha^2(w-c)} = i\frac{TG\pi}{\gamma M_e^2(w-c)}, \tag{32}$$

$$F = -\frac{T}{\gamma M_e^2(w-c)}\left(\pi + \frac{w'\pi'}{\alpha^2(w-c)}\right) = -\frac{T\pi}{\gamma M_e^2(w-c)}\left(1+\frac{w'G}{(w-c)}\right), \tag{33}$$

$$\Theta = T\left[\frac{\gamma-1}{\gamma}\pi - \frac{T'\pi'}{\gamma M_e^2\alpha^2(w-c)^2}\right] = T\pi\left[\frac{\gamma-1}{\gamma} - \frac{T'G}{\gamma M_e^2(w-c)^2}\right]. \tag{34}$$

For further discussion of amplitude distributions, the reader is referred to § 3.4.

3.2. *Viscous solutions*

No previous investigator has attempted to obtain analytical solutions of the full viscous equations, even at low Mach numbers. The present analysis is no exception. In order to bring out the differences between the present analysis and earlier studies, the assumptions and consequences of the Lees–Lin (1946) and Dunn–Lin (1955) analyses will first be reviewed briefly. The usual procedure in obtaining viscous solutions has been to solve a set of reduced equations that retain terms up to a certain order, either near the critical point or else near the surface. These sets of reduced equations are the same only if the surface is very close to the critical point. In fact this limitation applies to the Lees–Lin (1946) theory, in which a solution is obtained by convergent series expansion about the critical point and is then utilized to satisfy the surface boundary conditions. On the other hand the Dunn–Lin analysis assumes *a priori* that the wall is far from the critical layer and obtains a set of reduced equations valid near the wall but not at the critical layer.

The reduced equations of Lees & Lin (1946) and of Dunn & Lin (1955) are obtained by order-of-magnitude analyses. For the Lees–Lin case the ordering of terms is as follows:

$$\bar{Q}, \bar{Q}' \sim 1, \quad d/dy \sim 1/\epsilon, \quad (w-c) \sim \epsilon, \quad f \sim 1, \quad \phi \sim \epsilon f, \quad \theta \sim f, \quad \pi \sim \epsilon^3 f. \tag{35}$$

It must be remembered that the ordering relation $d/dy \sim 1/\epsilon$ is valid only in a restricted region. The leading terms of the disturbance equations under assumptions (35) form the following differential equations. These equations will be referred to as the Lees–Lin equations

$$f''' - i\alpha Re\nu^{-1}(w-c)f' = 0, \tag{36}$$

$$\phi' + if = 0, \tag{37}$$

$$\theta'' - i\alpha Re\sigma\nu^{-1}(w-c)\theta = \alpha Re\sigma\nu^{-1}T'\phi, \tag{38}$$

and

$$\epsilon \sim (\alpha Re)^{-\frac{1}{3}}. \tag{39}$$

Equations (36) to (38) are a sixth-order system of ordinary differential equations dependent only on the parameter αRe. It is to be noted, however, that the continuity and momentum equations (37) and (36) are a closed fourth-order set

independent of the energy equation; in fact, it is the same set that is obtained for incompressible flow. As will be shown in § 3.3, this independence makes possible the determination of the stability characteristics from the velocity fluctuation boundary conditions alone; the temperature fluctuations are irrelevant in this case.

Dunn & Lin (1955) recognized that, for supersonic flows, the propagation velocity c may be some substantial portion of the free-stream velocity, and the critical point may be relatively far from the wall. Accordingly, they ordered the various quantities occurring in the stability equations in the following manner

$$\bar{Q}, \bar{Q}' \sim 1, \quad d/dy \sim 1/\epsilon, \quad (w-c) \sim 1, \quad f \sim 1 \quad \phi \sim \epsilon f, \quad \theta \sim f, \quad \pi \sim \epsilon^2 f. \tag{40}$$

The leading terms of the disturbance equations under the ordering (40) form the Dunn–Lin viscous equations:

$$f''' - i\alpha Re\nu^{-1}(w-c)f' = 0, \tag{41}$$

$$\phi' + if = i(w-c)\theta/T, \tag{42}$$

$$\theta'' - i\alpha Re\sigma\nu^{-1}(w-c)\theta = 0, \tag{43}$$

and

$$\epsilon \sim (\alpha Re)^{-\frac{1}{2}}. \tag{44}$$

These equations also depend only on the one parameter αRe. The momentum and energy equations (41) and (43) are mutually independent while the normal velocity fluctuations are related to the longitudinal velocity fluctuations and the temperature fluctuations through the continuity equation (42).

The method of solution of equations (41) to (43) is given by Dunn (1953). He transforms equations (41) and (43) by introducing new variables of the form suggested by Tollmien (1947), so that the equations reduce to the form solved by Lees & Lin. The details of the transformation and the solutions of the Dunn & Lin equations are reviewed in Appendix D of Reshotko (1960) and also in Mack (1960). For $\alpha Rec \gg 1$, it is useful to obtain asymptotic solutions to the viscous disturbance equations. These solutions have in fact already been obtained by Dunn (1953). However, in most cases αRec is not sufficiently large to warrant the use of the asymptotic solutions, so that they are omitted from the present discussion.

As the Mach number of the flow increases, certain terms of the disturbance equations that are Mach-number-dependent grow larger than indicated by an ordering procedure based solely on free-stream Reynolds number. The normal gradient of mean temperature is of order M_e^2, and the inviscid amplitude relations (33) and (34) show that the 'inviscid' temperature fluctuations normalized with the free-stream temperature are also of order M_e^2, compared with the normalized longitudinal velocity fluctuations. The 'viscous' temperature fluctuations must therefore also be of order M_e^2. At the same time the whole mean temperature level in the boundary layer grows as M_e^2, and the free-stream static temperature level is no longer relevant. Temperature fluctuations and mean quantities that are temperature dependent should be normalized by some representative temperature $T_{\text{ref}} \sim M_e^2 T_e$. As shown by Dunn (1953), the new normalizations and new definitions of Mach number and Reynolds number are

$$\theta = \frac{\theta^*}{T^*_{\text{ref}}}, \quad T = \frac{T^*}{T^*_{\text{ref}}}, \quad M_{\text{ref}} = \frac{M_e}{\sqrt{T_{\text{ref}}}}, \quad Re_{\text{ref}} = \frac{Re}{\nu_{\text{ref}}}. \tag{45}$$

Even with the new temperature normalization, normal gradients of mean temperature-dependent quantities are of magnitude M_{ref}^2 times the normal mean velocity gradient. In general, $M_{\text{ref}} = O(1)$, so that the retention of M_{ref} in the ordering relations that follow is mainly for the purpose of identifying the terms depending on mean temperature gradient and the dissipation terms. The ordering relations used in the present analysis are as follows:

$$\bar{Q}, \bar{Q}' \sim 1 \text{ (except } T', \mu' \sim M_{\text{ref}}^2), \quad d/dy \sim 1/\bar{\epsilon},$$
$$f \sim 1, \ \theta \sim f, \ \phi \sim \bar{\epsilon} f, \ \pi \sim \bar{\epsilon}^2 f, \tag{46}$$

so that the orders of the terms in the disturbance equations may be grouped as follows:

$1, \ \bar{\epsilon}, \ M_{\text{ref}}^2 \bar{\epsilon}, \ M_{\text{ref}}^2 \bar{\epsilon}^2$ (αRe_{ref}) dependence only;

$\bar{\epsilon}^2, \ \bar{\epsilon}^3, \ M_{\text{ref}}^2 \bar{\epsilon}^3, \ \bar{\epsilon}^4, \ M_{\text{ref}}^2 \bar{\epsilon}^4$ α and (αRe_{ref}) dependence.

Here
$$\bar{\epsilon} \sim \frac{1}{(\alpha Re_{\text{ref}})^{\frac{1}{2}}} = \frac{(\nu_{\text{ref}})^{\frac{1}{2}}}{(\alpha Re)^{\frac{1}{2}}} \sim (\nu_{\text{ref}})^{\frac{1}{2}} \epsilon.$$

Terms in the disturbance equations arising from the fluctuating viscous stresses, heat-flux gradients, and viscous dissipation that are regarded of order ϵ in the Lees–Lin and Dunn–Lin analyses are actually of order $\bar{\epsilon}$. For a linear viscosity-temperature relation, $\bar{\epsilon} \sim M_e^2 \epsilon$, and at high supersonic and hypersonic Mach numbers, the above-mentioned terms are likely to be comparable in magnitude to the terms of unit order.

Referring to the grouping of ordered terms, no major difficulties arise when terms of order 1, $\bar{\epsilon}$, $M_{\text{ref}}^2 \bar{\epsilon}$, and $M_{\text{ref}}^2 \bar{\epsilon}^2$ are considered, since these depend only on the single parameter (αRe_{ref}). But if terms of order $M_{\text{ref}}^2 \bar{\epsilon}^2$ are to be included in the viscous equations, then to be consistent one should also include the pressure-fluctuation terms (of order $\bar{\epsilon}^2$) in the continuity and energy equations, and also the terms of order $\bar{\epsilon}^2$ with coefficient α^2 arising from the streamwise gradients of fluctuating quantities. In the present analysis only terms of order 1, $\bar{\epsilon}$, and $M_{\text{ref}}^2 \bar{\epsilon}$ are retained in order to investigate the first-order effects of viscous dissipation and large mean normal temperature gradients, hitherto neglected.

The viscous disturbance equations here considered are as follows:

Momentum:
$$f''' + \frac{2}{\mu}\frac{d\mu}{dT} T' f'' + \frac{1}{\mu}\frac{d\mu}{dT} w' \theta'' + \frac{i\alpha Re(w-c)}{\nu}\left(\frac{T'}{T} f - f' - \frac{w'}{T}\theta\right) = 0. \tag{47}$$

Continuity:
$$\phi' + if - \frac{T'}{T}\phi - \frac{i(w-c)}{T}\theta = 0. \tag{48}$$

Energy:
$$\theta'' + \frac{2}{\mu}\frac{d\mu}{dT} T' \theta' + 2(\gamma - 1)\sigma M_e^2 w' f' - \frac{i\alpha Re\sigma(w-c)}{\nu}\theta = \frac{\sigma \alpha Re T'}{\nu}\phi. \tag{49}$$

In contrast to the Lees–Lin and Dunn–Lin viscous equations, the current set [equations (47) to (49)] have no independence properties, and the three equations

must be solved simultaneously. The linearly independent solutions to equations (47) to (49) are distinguished by their behaviour in the outer flow where mean flow quantities have reached their external values. In the outer flow, equations (47) to (49) become

$$f''' - i\alpha Re(1-c)f' = 0, \tag{50}$$

$$\phi' + if = i(1-c)\theta, \tag{51}$$

and

$$\theta'' - i\alpha Re\sigma(1-c)\theta = 0. \tag{52}$$

One set of solutions to equations (50) to (52) is of the form

$$f' \sim \exp[\pm\{i\alpha Re(1-c)\}^{\frac{1}{2}} y], \quad \theta = 0, \tag{53}$$

while another set is of the form

$$\theta \sim \exp[\pm\sqrt{\{i\alpha Re\sigma(1-c)\}^{\frac{1}{2}}} y], \quad f = 0. \tag{54}$$

A third set corresponding to $f' = 0$ is replaced by the inviscid solution and is therefore not considered here. In equations (53) and (54) the solutions with the positive exponents are rejected immediately, since they grow exponentially and cannot possibly satisfy the outer boundary condition [equation (10)]. The remaining two sets of solutions corresponding to the negative exponents must now be found. Since equations (47) to (49) are rather tightly coupled, it is likely that their simultaneous solution will have to be obtained numerically. The method is somewhat similar to that used to obtain the inviscid solution.

Consider the solution corresponding to the negative exponent in equation (54). Let

$$H \equiv \theta'/\theta, \quad J \equiv \phi/\theta, \quad K \equiv f/\theta. \tag{55}$$

In terms of H, J, and K, equations (47) to (49) become

$$H' = -\frac{2}{\mu}\frac{d\mu}{dT}T'H - 2(\gamma-1)\sigma M_e^2 w'(K'+HK) + \frac{i\alpha Re\sigma(w-c)}{\nu} + \frac{\sigma\alpha ReT'}{\nu}J - H^2, \tag{56}$$

$$J' = -iK + \frac{i(w-c)}{T} + \frac{T'}{T}J - HJ, \tag{57}$$

$$\begin{aligned} K''' = {} & -\frac{2}{\mu}\frac{d\mu}{dT}T'[K'' + H(2K'+HK) + H'K] - \frac{1}{\mu}\frac{d\mu}{dT}w'(H'+H^2) \\ & - \frac{i\alpha Re(w-c)}{\nu}\left[\frac{T'}{T}K - (K'+HK) - \frac{w'}{T}\right] \\ & - H(3K'' + 3K'H + 3H'K + H^2K) - 3K'H' - H''K, \end{aligned} \tag{58}$$

with 'outer' conditions

$$H_0 = -\{i\alpha Re\sigma(1-c)\}^{\frac{1}{2}}, \quad J_0 = -\{i(1-c)/\alpha Re\sigma\}^{\frac{1}{2}}, \quad K_0 = 0. \tag{59}$$

The equations for the set corresponding to the negative exponent in equation (53) are obtained in a similar manner. With

$$L \equiv \phi/f, \quad M \equiv f'/f, \quad N \equiv \theta/f, \tag{60}$$

equations (47) to (49) become

$$L' = -i + \frac{i(w-c)}{T} N + \frac{T'}{T} L - LM, \tag{61}$$

$$M'' = -\frac{2}{\mu}\frac{d\mu}{dT} T'(M' + M^2) - \frac{1}{\mu}\frac{d\mu}{dT} w'[N'' + (2N' + NM)M + NM'] - \frac{i\alpha Re(w-c)}{\nu}\left(\frac{T'}{T} - M - \frac{w'}{T} N\right) - M(3M' + M^2), \tag{62}$$

$$N'' = -\frac{2}{\mu}\frac{d\mu}{dT} T'(N' + NM) - 2(\gamma - 1)\sigma M_e^2 w' M + \frac{i\alpha Re\sigma(w-c)}{\nu} N + \frac{\sigma\alpha Re}{\nu} T' L - (2N' + NM)M - NM', \tag{63}$$

and the outer conditions are

$$L_0 = \{i/\alpha Re(1-c)\}^{\frac{1}{2}}, \quad M_0 = -\{i\alpha Re(1-c)\}^{\frac{1}{2}}, \quad N_0 = 0. \tag{64}$$

The '*HJK*' and '*LMN*' systems of equations are separated into their component real and imaginary equations and are then integrated from the outer edge of the boundary layer to the wall for two main reasons: (1) the outer conditions are known; (2) the outer region behaves as a saddle point in the sense that integral curves other than those satisfying the outer condition diverge from the outer condition.†

3.3. *Eigenvalue problem*

Having indicated the methods of obtaining the various solutions of the disturbance equations, the solutions must be combined to satisfy the boundary conditions. Note that the outer boundary conditions for subsonic disturbances [equation (10)] are inherently satisfied by choosing the negative exponents in equations (21), (53), and (54).‡ The three boundary conditions at the wall remain to be satisfied. They are $f_w = \phi_w = \theta_w = 0$.

Following the pattern of Dunn & Lin (1955), the inviscid functions in this section will be capitalized, while the functions corresponding to the *LMN* solution will be given the subscript 3, and those corresponding to the *HJK* system the subscript 5.

The satisfaction of the boundary conditions leads to the following determinantal relation

$$\begin{vmatrix} \Phi_w & \phi_{3w} & \phi_{5w} \\ F_w & f_{3w} & f_{5w} \\ \Theta_w & \theta_{3w} & \theta_{5w} \end{vmatrix} = 0, \tag{65}$$

which, when expanded, yields the secular equation

$$\frac{\Phi_w}{F_w} = \frac{\phi_{3w}}{f_{3w}} + \frac{\Theta_w}{F_w}\left(\frac{\phi_{5w}}{\theta_{5w}} - \frac{\phi_{3w}}{f_{3w}}\frac{f_{5w}}{\theta_{5w}}\right) + \frac{\Phi_w}{F_w}\frac{\theta_{3w}}{f_{3w}}\frac{f_{5w}}{\theta_{5w}} - \frac{\theta_{3w}}{f_{3w}}\frac{\phi_{5w}}{\theta_{5w}}. \tag{66}$$

† This behaviour is shown in Appendix E of Reshotko (1960).

‡ The process of patching two independent inviscid solutions at the outer boundary by the condition $\phi' + \alpha\{1 - M_e^2(1-c)^2\}^{\frac{1}{2}}\phi = 0$, which is required in the Lees–Lin and Dunn–Lin procedures, is here unnecessary.

Note that in the Lees–Lin, Dunn–Lin, and present formulations the inviscid solutions depend only on the parameter α while the viscous solutions depend only on αRe. With the aid of the following identity, derived from the inviscid equations (12) and (14),

$$\frac{\Theta_w}{F_w} = (\gamma-1)M_e^2 c + i(\gamma-1)M_e^2 c\left[\frac{w'_w}{c} - \frac{T'_w}{(\gamma-1)M_e^2 c^2}\right]\frac{\Phi_w}{F_w}, \tag{67}$$

equation (66) can be written

$$\frac{\Phi_w}{F_w} = \frac{\dfrac{\phi_{3w}}{f_{3w}} + \dfrac{\phi_{5w}}{\theta_{5w}}\left[(\gamma-1)M_e^2 c - \dfrac{\theta_{3w}}{f_{3w}}\right] - (\gamma-1)M_e^2 c\dfrac{\phi_{3w}}{f_{3w}}\dfrac{f_{5w}}{\theta_{5w}}}{1 - i(\gamma-1)M_e^2 c\dfrac{\phi_{5w}}{\theta_{5w}}\left[\dfrac{w'_w}{c} - \dfrac{T'_w}{(\gamma-1)M_e^2 c^2}\right] + \dfrac{f_{5w}}{\theta_{5w}}\left\{i(\gamma-1)M_e^2 c\dfrac{\phi_{3w}}{f_{3w}}\left[\dfrac{w'_w}{c} - \dfrac{T'_w}{(\gamma-1)M_e^2 c^2}\right] - \dfrac{\theta_{3w}}{f_{3w}}\right\}}. \tag{68}$$

The Lees–Lin and Dunn–Lin secular equations are also quite simply obtained. For the Lees–Lin viscous solutions, $\phi_5 = f_5 = 0$. Since θ_{5w} is generally not zero, equation (68) becomes

$$\Phi_w/F_w = \phi_{3w}/f_{3w}. \tag{69}$$

This result confirms the irrelevance of the thermal boundary condition in the Lees–Lin case.

For the Dunn–Lin solution, $\theta_3 = f_5 = 0$, so that the secular equation is

$$\frac{\Phi_w}{F_w} = \frac{\dfrac{\phi_{3w}}{f_{3w}} + (\gamma-1)M_e^2 c\dfrac{\phi_{5w}}{\theta_{5w}}}{1 - i(\gamma-1)M_e^2 c\dfrac{\phi_{5w}}{\theta_{5w}}\left[\dfrac{w'_w}{c} - \dfrac{T'_w}{(\gamma-1)M_e^2 c^2}\right]}. \tag{70}$$

For some unstated reason, Dunn & Lin (1955) apparently omitted the second term on the right side of equation (67) so that the denominator of equation (70) in their formation is simply unity. This omission is here corrected.

In the terminology of the present method (§ 3.2), equation (68) may be written

$$\Phi_w/F_w = \mathscr{R}, \tag{71}$$

where

$$\mathscr{R} = \frac{L_w + J_w[(\gamma-1)M_e^2 c - N_w] - (\gamma-1)M_e^2 c L_w K_w}{1 - i(\gamma-1)M_e^2 c J_w\left[\dfrac{w'_w}{c} - \dfrac{T'_w}{(\gamma-1)M_e^2 c^2}\right] + K_w\left\{i(\gamma-1)M_e^2 c L_w\left[\dfrac{w'_w}{c} - \dfrac{T'_w}{(\gamma-1)M_e^2 c^2}\right] - N_w\right\}}. \tag{72}$$

Again, from the inviscid equations (11) to (14),

$$\frac{\Phi_w}{F_w} = \frac{i}{\{(w'_w/c) - (1/G_w)\}}, \tag{73}$$

so that relation (68) may finally be written

$$G_w = (c/w'_w)(1-\psi), \tag{74}$$

where

$$\psi \equiv (1 + iw'_w\mathscr{R}/c)^{-1}. \tag{75}$$

In equation (74), G_w depends on α alone, while the right side depends on αRe alone. The values of α and αRe for which equation (74) is satisfied are the desired characteristic values. Some detailed examples of this procedure are given in § 4.

3.4. *Amplitude distributions*

Once the characteristic values of α and Re are determined, the distributions of the amplitudes of the disturbance quantities across the boundary layer are calculated by obtaining the amplitude distributions for the inviscid solutions, the LMN solutions (solutions 3) and the HJK solutions (solutions 5) and combining them in the manner satisfying the boundary conditions. The discussion in this section concerns the functions π, ϕ, f, and θ. The normal velocity fluctuations are given by $\alpha\phi$, while the density fluctuation amplitude can be obtained by using the equation of state.

Before proceeding, it must be recalled that, in splitting the solutions into inviscid and viscous types, a singularity was artificially introduced into the inviscid equations at the critical point by the complete elimination of viscous and heat-conduction effects from these equations (§ 3.1). Accordingly, before using the inviscid solutions in composing the amplitude distributions, they must be corrected for the effects of viscosity and thermal conductivity in the neighbourhood of the critical layer. For incompressible flow, such corrections were first obtained by Tollmien (1947) and Schlichting (1935).

Here we seek the leading viscous corrections to the inviscid functions in the region about the critical point. To be more specific, the corrected function is given by

$$q_{\text{corr}} = q_{\text{inv}} - (\text{singular term}) + (\text{viscous replacement term}),$$

where the viscous replacement function is obtained by solving the disturbance equation containing only the leading viscous terms in the neighbourhood of the critical point. This replacement function must satisfy the condition that 'far' away from the critical layer it approaches asymptotically the singular portion of the original uncorrected inviscid function.

The behaviour of the uncorrected inviscid functions in the neighbourhood of the critical layer is obtained from a series expansion of the inviscid solution around the critical point. The series expansion for the pressure fluctuation amplitude has already been obtained [equations (26) to (29)]. The other inviscid amplitudes are related to π and π' through equations (32) to (34). The results for Φ, F, and Θ are respectively as follows.

Normal velocity fluctuation amplitude function Φ

For $(y-y_c) > 0$,

$$\Phi = -\frac{i}{\gamma M_e^2}\frac{T_c}{w_c'}\left\{1 + A(y-y_c)\ln(y-y_c) + \left[\left(\frac{T_c'}{T_c} - \frac{w_c''}{2w_c'}\right) - \text{const.}\right](y-y_c) + \ldots\right\}. \quad (76)$$

For $(y-y_c) < 0$,

$$\Phi = -\frac{i}{\gamma M_e^2}\frac{T_c}{w_c'}\left\{1 + A(y-y_c)\ln|y-y_c| + \left[\left(\frac{T_c'}{T_c} - \frac{w_c''}{2w_c'}\right) - \text{const.}\right](y-y_c) + \ldots\right\}$$
$$- \frac{1}{\gamma M_e^2}\frac{T_c}{w_c'} A\pi(y-y_c) + \ldots. \quad (77)$$

The quantity A is the derivative of the density-vorticity product at the critical point as defined by equation (28). When $A = 0$, there are no discontinuities in Φ. For $A \neq 0$, the values of Φ_r and Φ_i are continuous, but Φ_r is discontinuous in slope at the critical point, while Φ_i has a discontinuity in curvature.

Longitudinal velocity fluctuation amplitude function F

For $(y-y_c) > 0$,

$$F = \frac{1}{\gamma M_e^2}\frac{T_c}{w_c'}\left\{A\ln(y-y_c)+\left[\frac{w_c''}{2w_c'}-\text{const.}\right]+\ldots\right\}. \tag{78}$$

For $(y-y_c) < 0$,

$$F = \frac{1}{\gamma M_e^2}\frac{T_c}{w_c'}\left\{A\ln|y-y_c|+\left[\frac{w_c''}{2w_c'}-\text{const.}\right]+\ldots\right\}-\frac{i}{\gamma M_e^2}\frac{T_c}{w_c'}A\pi+\ldots. \tag{79}$$

There are no discontinuities in F for $A = 0$. However, for $A \neq 0$, F_r has a logarithmic infinity while there is a jump discontinuity in F_i.

Temperature fluctuation amplitude function Θ

For $(y-y_c) > 0$,

$$\Theta = \frac{1}{\gamma M_e^2}\frac{T_c T_c'}{w_c'^2}\left\{\frac{1}{(y-y_c)}+A\ln(y-y_c)+\left[\frac{T_c'}{T_c}+\frac{(\gamma-1)M_e^2 w_c'}{T_c'}-A-\text{const.}\right]+\ldots\right\}. \tag{80}$$

For $(y-y_c) < 0$,

$$\Theta = \frac{1}{\gamma M_e^2}\frac{T_c T_c'}{w_c'^2}\left\{\frac{1}{(y-y_c)}+A\ln|y-y_c|+\left[\frac{T_c'}{T_c}+\frac{(\gamma-1)M_e^2 w_c'}{T_c'}-A-\text{const.}\right]+\ldots\right\} -\frac{i}{\gamma M_e^2}\frac{T_c T_c'}{w_c'^2}A\pi+\ldots. \tag{81}$$

To be noted immediately is the $1/(y-y_c)$ discontinuity in Θ_r even for $A = 0$. This irregularity in the distribution of temperature-fluctuation amplitude is caused simply by the assumed absence of thermal conduction. For $A \neq 0$, there is an additional logarithmic discontinuity in Θ_r and a jump discontinuity in Θ_i. The inviscid disturbance vorticity given by $(F''+i\alpha^2\Phi)$ has a discontinuity similar to that of the temperature fluctuations.

The corrections for viscosity and conductivity are introduced logically using the method of convergent series expansion about the critical point as developed by Lees & Lin (1946) and Cheng (1953). In the present case this expansion is carried out in the Tollmien variable. Furthermore, the present development (see Reshotko 1960) reduces the correction equations to the forms solved by Schlichting (1935), so that the universal functions first calculated by Schichting (1935) and later improved by Holstein (1950) could be used here. Consider, for example, the corrections to Θ_r. The function $(\Theta_r)_{\text{corr}}$ may be expressed as

$$(\Theta_r)_{\text{corr}} = \Theta_r - (\text{singular terms}) + (\text{viscous replacement terms}). \tag{82}$$

The singular terms from equation (81) are

$$\frac{1}{\gamma M_e^2}\frac{T_c T_c'}{w_c'^2}\left[\frac{1}{(y-y_c)}+A\ln|y-y_c|\right]. \tag{83}$$

The replacement terms (see Appendix G, Reshotko 1960) are

$$\frac{1}{\gamma M_e^2}\frac{T_c T_c'}{w_c'^2}\left\{\frac{1}{(y-y_c)}\zeta_0\hat{G}''(\zeta_0)+A\left[\hat{G}'(\zeta_0)-\ln\frac{|\zeta_0|}{|y-y_c|}\right]\right\}, \tag{84}$$

where

$$\zeta_0 = (\alpha Re)^{\frac{1}{3}} Y_0 \tag{85}$$

ζ	$\hat{G}'(\zeta)$	$\hat{G}''(\zeta)$	$\hat{H}'(\zeta)$
−8·0	2·0795	−0·1250	−3·1429
−7·5	2·0149	−0·1333	−3·1432
−7·0	1·9460	−0·1428	−3·1435
−6·5	1·8719	−0·1538	−3·1440
−6·0	1·7919	−0·1668	−3·1444
−5·5	1·7052	−0·1801	−3·1445
−5·0	1·6107	−0·1936	−3·1447
−4·5	1·5110	−0·2105	−3·1479
−4·0	1·3990	−0·2419	−3·1592
−3·5	1·2633	−0·3082	−3·1839
−3·0	1·0817	−0·4281	−3·2192
−2·5	0·8268	−0·5969	−3·2424
−2·0	0·4845	−0·7657	−3·2047
−1·5	0·0760	−0·8454	−3·0433
−1·0	−0·3309	−0·7475	−2·7067
−0·5	−0·6366	−0·4434	−2·1944
0	−0·7506	0	−1·5708
0·5	−0·6366	0·4434	−0·9472
1·0	−0·3309	0·7475	−0·4349
1·5	0·0760	0·8454	−0·0983
2·0	0·4845	0·7657	0·0631
2·5	0·8268	0·5969	0·1008
3·0	1·0817	0·4281	0·0776
3·5	1·2633	0·3082	0·0423
4·0	1·3990	0·2419	0·0176
4·5	1·5110	0·2105	0·0063
5·0	1·6107	0·1936	0·0031
5·5	1·7052	0·1801	0·0029
6·0	1·7919	0·1668	0·0028
6·5	1·8719	0·1538	0·0024
7·0	1·9460	0·1428	0·0019
7·5	2·0149	0·1333	0·0016
8·0	2·0795	0·1250	0·0013

TABLE 1. Viscous correction functions (from Holstein 1950).

The Tollmien variable for the energy equation is defined by

$$Y_0 \equiv \left[\int_{y_c}^{y}\frac{3}{2}\left\{\frac{\sigma(w-c)}{\nu}\right\}^{\frac{1}{2}}dy\right]^{\frac{2}{3}}, \tag{86}$$

and the functions $\hat{G}''(\zeta_0)$ and $\hat{G}'(\zeta_0)$ are the functions calculated and presented by Holstein (1950) and reproduced here (table 1). Combining equations (82), (83) and (84), we have

$$(\Theta_r)_{\text{corr}} = \Theta_r - \frac{1}{\gamma M_e^2}\frac{T_c T_c'}{w_c'^2}\left\{\frac{1}{(y-y_c)}[1-\zeta_0\hat{G}''(\zeta_0)]+A[\ln|\zeta_0|-\hat{G}'(\zeta_0)]\right\}. \tag{87}$$

The thickness of the viscous conductive region is approximately $-4 < \zeta_0 < 4$. Accordingly, the braced term in equation *(87)* becomes very small for $|\zeta_0| > 4$, so that outside the region $(\Theta_r)_{\text{corr}} \approx \Theta_r$.

Following the same principle, the corrected forms for Θ_i, F_r, and F_i are:

For $(y - y_c) < 0$,

$$(\Theta_i)_{\text{corr}} = \Theta_i + \frac{A}{\gamma M_e^2} \frac{T_c T'_c}{w'^2_c} [\pi + \hat{H}'(\zeta_0)]. \tag{88a}$$

For $(y - y_c) > 0$,

$$(\Theta_i)_{\text{corr}} = \frac{A}{\gamma M_e^2} \frac{T_c T'_c}{w'^2_c} \hat{H}'(\zeta_0); \tag{88b}$$

$$(F_r)_{\text{corr}} = F_r - \frac{A}{\gamma M_e^2} \frac{T_c}{w'_c} [\ln |\zeta| - \hat{G}'(\zeta)]. \tag{89}$$

For $(y - y_c) < 0$,

$$(F_i)_{\text{corr}} = F_i + \frac{A}{\gamma M_e^2} \frac{T_c}{w'_c} [\pi + \hat{H}'(\zeta)]. \tag{90a}$$

For $(y - y_c) > 0$,

$$(F_i)_{\text{corr}} = \frac{A}{\gamma M_c^2} \frac{T_c}{w'_c} \hat{H}'(\zeta), \tag{90b}$$

where

$$\zeta = (\alpha Re)^{\frac{1}{3}} Y, \tag{91}$$

and

$$Y = \left(\int_{y_c}^{y} \frac{3}{2} \left\{ \frac{w - c}{\nu} \right\}^{\frac{1}{2}} dy \right)^{\frac{2}{3}}. \tag{92}$$

The preceding corrections are the important ones. The largest correction is to the function Θ_r and must be made whether or not A vanishes. All the other corrections are directly proportional to the value of A, which is usually small. Even smaller are the corrections to Φ_r, which is continuous in value but has an infinite slope at the critical point, and the corrections to π_r where the irregularity does not appear until the third derivative. The corrections to Φ and π are not obtained here. For incompressible flow, temperature fluctuations are irrelevant and all the corrections are likely to be small.

The amplitudes of the viscious solutions are obtained as follows:

$$f_3 = \exp\left(\int_0^y M \, dy \right) = \exp\left(\int_0^y M_r \, dy \right) \left\{ \cos\left(\int_0^y M_i \, dy \right) + i \sin\left(\int_0^y M_i \, dy \right) \right\}, \tag{93}$$

$$\phi_3 = L f_3, \tag{94}$$

$$\theta_3 = N f_3. \tag{95}$$

Similarly,

$$\theta_5 = \exp\left(\int_0^y H \, dy \right) = \exp\left(\int_0^y H_r \, dy \right) \left\{ \cos\left(\int_0^y H_i \, dy \right) + i \left(\sin \int_0^y H_i \, dy \right) \right\}, \tag{96}$$

$$\phi_5 = J \theta_5, \tag{97}$$

$$f_5 = K \theta_5. \tag{98}$$

Since all the solutions are eigenfunctions and also satisfy the outer boundary conditions, the proper linear combination is determined by satisfying two of the

boundary conditions at the wall. Except for an arbitrary scaling factor, the resulting expressions for the amplitude distributions can be written

$$\phi = (\Phi + b_3\phi_3 + b_5\phi_5), \tag{99}$$

$$f = (F_{\text{corr}} + b_3 f_3 + b_5 f_5), \tag{100}$$

$$\theta = (\Theta_{\text{corr}} + b_3\theta_3 + b_5\theta_5), \tag{101}$$

$$\pi = \pi_{\text{inv}}, \tag{102}$$

where

$$b_3 = \frac{F_w - \Theta_w K_w}{N_w K_w - 1} \tag{103}$$

and

$$b_5 = \frac{\Theta_w - N_w F_w}{N_w K_w - 1}. \tag{104}$$

4. Examples

To illustrate the present methods and to help estimate their validity, several numerical examples were obtained for insulated flat-plate boundary layers. The particular mean flow profiles used in the examples are those computed by Mack (1958) using real-gas fluid properties. Mack's tables are particularly suited for stability calculations in that most of the derivatives of the profile functions required for the stability analysis are presented. The variable η used in this section is that defined by Mack, namely, $\eta = y^*(\overline{u_e^*}/\nu_e^* x^*)^{\frac{1}{2}}$, and is directly proportional to the physical distance normal to the wall. The values of α_θ and Re_θ are made dimensionless with η_θ, where η_θ is a constant whose value varies only slightly with Mach number. For $0 < M_e < 5$, $0{\cdot}641 < \eta_\theta < 0{\cdot}664$ (Mack 1958).

The integrations of the inviscid and viscous equations required for the examples were performed numerically on the Datatron 205 of the Caltech Computing Center using a Runge–Kutta integration method.

4.1. *Neutral inviscid oscillations at $\alpha Re \to \infty$*

The necessary and sufficient condition for the existence of a neutral purely inviscid oscillation ($\alpha Re \to \infty$) is that (Lees & Lin 1946)

$$A \equiv \left(\frac{w_c''}{w_c'} - \frac{T_c'}{T_c}\right) = 0 \quad \text{for} \quad c > [1 - (1/M_e)].$$

The value of the propagation velocity c for which this condition is satisfied is denoted c_s, and depends on the particular profile being studied. In addition to the expected sensitivity to Mach number and surface-temperature level, it is also quite sensitive to the Prandtl number and viscosity-temperature relationship, as indicated by the calculations of van Driest (1952). Figure 4 shows the variation of c_s with Mach number at different surface-temperature levels. Also shown on figure 4 is the curve $c = [1 - (1/M_e)]$. The disturbance propagation velocity for supersonic and hypersonic boundary layers is a very substantial portion of the free-stream velocity, and the critical layer (where $w = c$) cannot be thought of as being close to the wall.

For the mean boundary-layer profiles of Mack (1958), the wave numbers corresponding to $A = 0$, $c = c_s$ were obtained for Mach numbers between 1·3 and

5·6 and are shown in figure 5. The value of $\alpha_{s\theta}$ increases in the subsonic range and (after a dip near $M_e = 1{\cdot}6$) reaches a peak at about Mach number 5 and then decreases with further rise in Mach number.The approximate behaviour of $\alpha_{s\theta}$ for very large Mach number was obtained for $\rho\mu$ = const., Prandtl number 1 by integrating equation (25) under the assumption that $M_e \gg 1$. The result shows

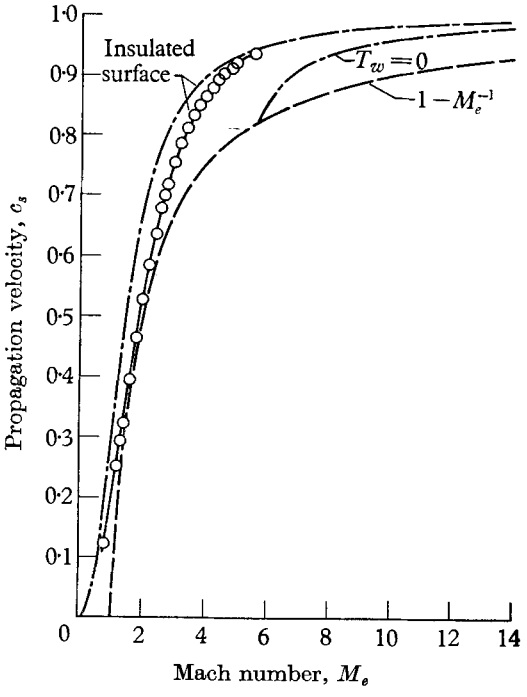

FIGURE 4. Propagation velocity of neutral inviscid disturbances for flat-plate boundary layers. — — —, $\rho\mu$ = const., $\sigma = 1$; ○, real gas profiles (Mack 1958), $T_0 = 100°$ F.

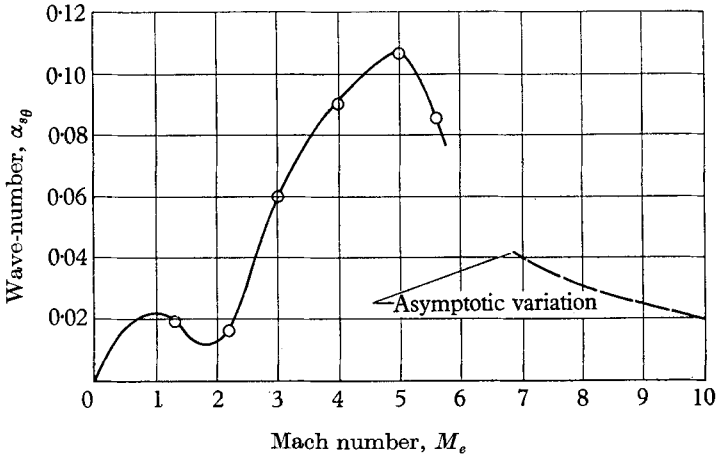

FIGURE 5. Wave-number of neutral inviscid oscillation. ○, Calculated points—real gas profiles (Mack 1958), $T_0 = 100°$ F; asymptotic variation, $\rho\mu$ = const., $\sigma = 1$, $\alpha_{s\theta} = 1{\cdot}97/M_e^2$.

that for very large Mach number $\alpha_{s_\theta} \sim 1/M_e^2$—a trend that seems to be consistent with the calculated points in figure 5. It might be expected that the wave-numbers obtained for neutral inviscid disturbances ($\alpha Re \to \infty$) at different Mach numbers would be somewhat indicative of the variation of the level of wave-number with Mach number for finite Reynolds numbers.

The variation of the function $G(y) = \pi'/\alpha^2\pi$ is shown in figure 6. In each case, the largest value of η for which $G = 0$ is the critical point. These curves have the general behaviour described in § 3.1. The integral under the curves is proportional

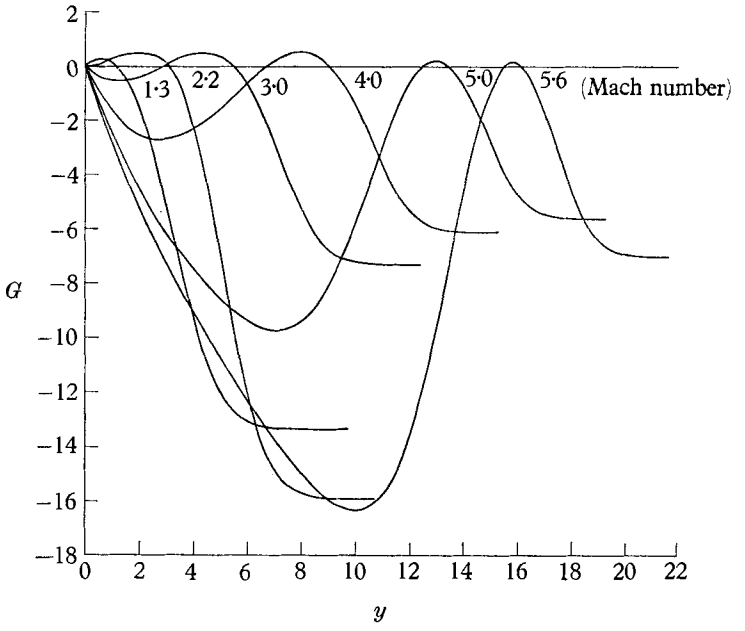

FIGURE 6. Distribution of $G = \pi'/\alpha^2\pi$ for neutral inviscid disturbance.

to the logarithm of the pressure fluctuation amplitude. Thus, if the net area under the G curve is positive, the pressure fluctuation amplitude is higher than the wall value; if the net area is negative, the pressure fluctuation level is below its wall value.

For each of the curves in figure 6, the pressure fluctuation amplitude at the critical point is calculated by the formula $\pi_c/\pi_w = \exp\left(\alpha^2 \int_0^{\eta_c} G\, d\eta\right)$. The results are shown in figure 7. For Mach numbers up to about 3, the pressure fluctuation level at the critical point is about the same as that at the wall, and is in fact quite constant in the region between the wall and the critical point. Above Mach 3, however, the pressure fluctuation level at the critical point drops quite sharply, and at Mach number 5·6 it is of the order of 6 % of the wall pressure-fluctuation level. This sharp drop occurs when the wall is supersonic with respect to the wave and is attributed to the rapid increase with Mach number in the amplitude of normal velocity fluctuations between the wall and the critical point. From normal momentum considerations, this large velocity fluctuation must be counter-

balanced by a large gradient in pressure fluctuation amplitude. Some further discussion of this point is given in § 5.

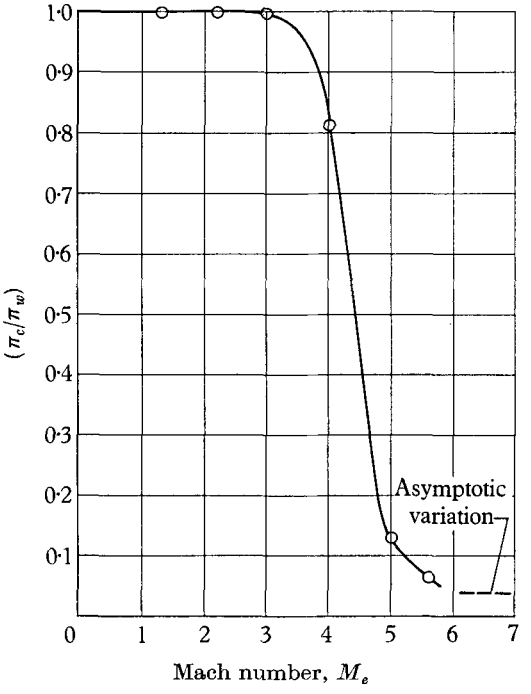

FIGURE 7. Pressure fluctuation amplitude at critical point, neutral inviscid oscillation: π_c/π_w, ratio of critical point to wall pressure-fluctuation amplitudes. ○, Calculated points—real gas profiles (Mack 1958), $T_0 = 100°$ F; asymptotic variation, $\rho\mu$ = const., $\sigma = 1$.

4.2. *Neutral stability characteristics of insulated supersonic boundary layers*

Using the insulated boundary-layer profiles of Mack (1958), neutral stability characteristics were calculated at Mach numbers of 2·2 and 5·6 to compare with the experimental findings of Laufer & Vrebalovich (1958, 1960) and with the Mach number 5·8 experiment of Demetriades (1958, 1960) respectively.

4.2.1. *Mach number* 2·2. At Mach number 2·2 the inviscid solutions for different values of c have imaginary parts that are almost completely independent of α and whose level increases monotonically with c. The neutral stability diagram is constructed as follows. At $c = c_s$, there are two solutions (see figure 8). The solution for which $\mathrm{Re}(\psi - 1) = \mathrm{Im}(\psi - 1) = 0$ represents the neutral inviscid oscillation, while that for $\mathrm{Re}(\psi - 1) \neq 0$ is a point on the lower branch. For $c > c_s$ (e.g. c_1, c_2, etc.) there are two solutions—one upper branch and one lower branch—until for $c = c_3$, the two solutions merge into one. For $c > c_3$ (e.g. c_4) there are no solutions, so that c_3 is the maximum value of c for a neutral disturbance. The remainder of the lower branch is composed of the single solutions for $[1 - (1/M_e)] < c < c_s$. The locus of all of these solutions is the familiar neutral-stability diagram.

The presently calculated neutral-stability diagram for Mach number 2·2 is shown in figure 9, together with the experimental points of Laufer & Vrebalovich (1958, 1960). There is good agreement between theory and experiment on the upper branch. On the lower branch, however, the experimental values of $\alpha_\theta Re_\theta$ are almost twice the theoretical values. The major reason for this difference is probably that $\bar{\epsilon}$ is too large† and that the higher-order terms omitted in formulating the viscous equations become important. Also shown in figure 9 as a dashed line is the neutral-stability loop calculated using the Lees–Lin viscous solutions. The upper branch of this loop is only slightly below that of the present

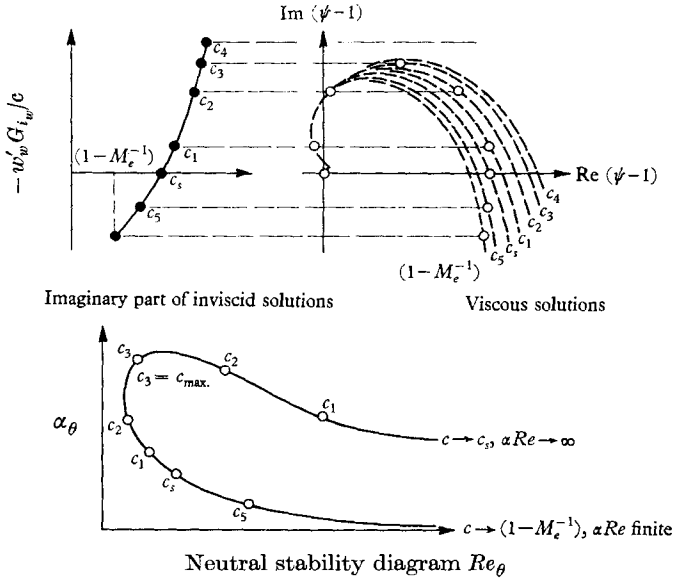

FIGURE 8. Schematic construction of neutral stability diagram at $M_e = 2{\cdot}2$.

theory, while the results of the two theories on the lower branch are almost coincident. Although not shown on the figure, the upper branch results of the present theory agree with those using the Dunn–Lin viscous solution (Mack 1960). On the lower branch, however, the Dunn–Lin results give the lowest values of αRe.

These results relative to the Lees–Lin theory may be explained qualitatively as follows. The improvement introduced in the Dunn–Lin theory is to take proper account of the effect of compressibility on the energy fed into the disturbance flow by the action of viscosity at the wall. As will be shown in the next section, the magnitude of this compressibility effect is related to a parameter $(M_e^2 c^2)/T_w$. This effect is always destabilizing, so that the Dunn–Lin neutral curve will always tend to be outside the Lees–Lin loop (figure 10). In the present theory, however, the effects of including the additional dissipation, shear, and conduction terms become noticeable on the lower branch (where αRe is small) and tend to push the lower-branch curve back toward the Lees–Lin curve, or even beyond it.

A set of disturbance amplitude distributions across the boundary layer was obtained for the upper-branch neutral point at $Re_\theta = 535$ and compared with a

† For the point on the lower branch where $\alpha_\theta = 0{\cdot}030$ and $Re_\theta = 89$, the value of $\bar{\epsilon}$ is 0·54.

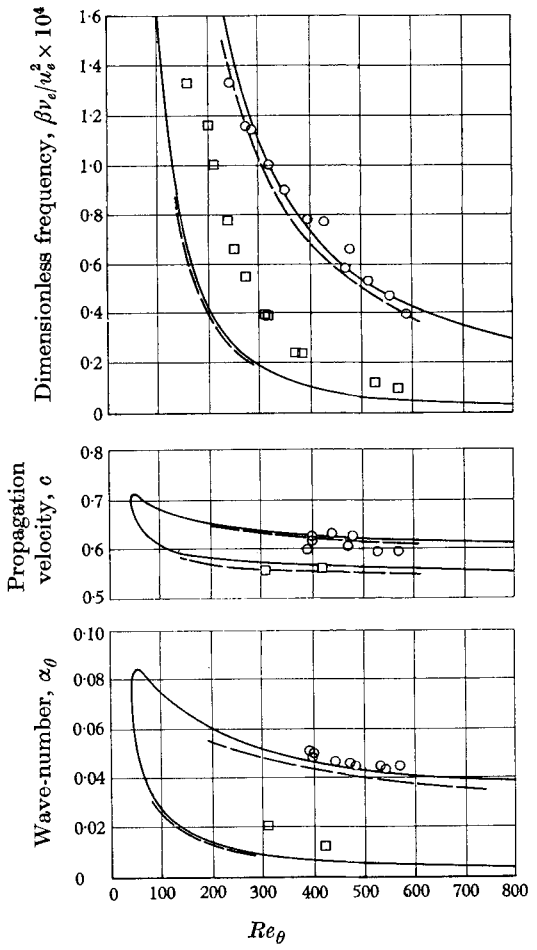

FIGURE 9. Neutral stability characteristics, $M_e = 2{\cdot}2$. ——, Present theory; — —, Lees–Lin theory (Mack). Laufer–Vrebalovich data: ○, upper branch; □, lower branch.

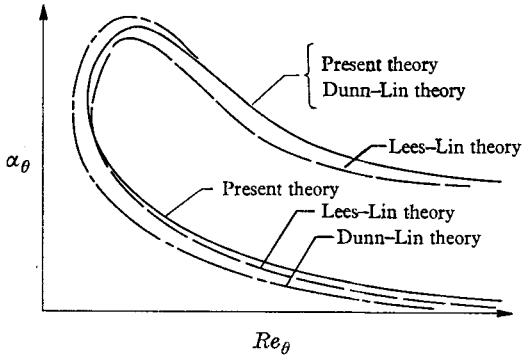

FIGURE 10. Schematic comparison at $M_e = 2{\cdot}2$ of neutral stability diagrams from Lees–Lin, Dunn–Lin, and present theories.

set of experimental distributions obtained by Laufer & Vrebalovich (1958, 1960) for the upper neutral point at $Re_\theta = 400$. The calculated disturbance amplitudes are scaled so as to match the experimental mass-flow fluctuation at δ. From figure 11, the agreement outward from the critical layer is seen to be quite good, while in the neighbourhood of the critical layer the agreement is perhaps not

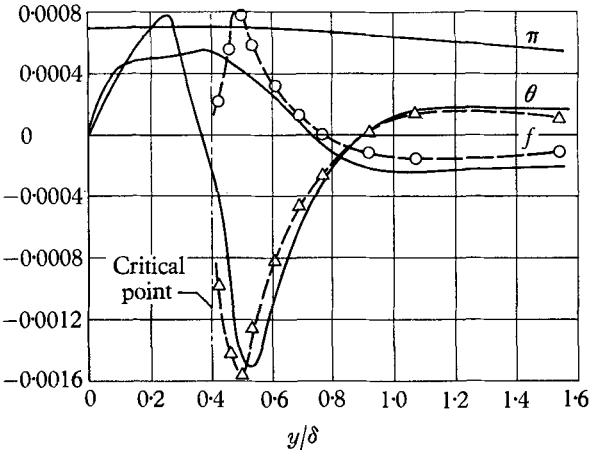

FIGURE 11. Amplitude distributions for neutral oscillation, $M_e = 2{\cdot}2$. ——, Present theory, $Re_\theta = 535$, $c = 0{\cdot}616$. Laufer–Vrebalovich data, $Re_\theta = 400$, $c = 0{\cdot}62$: --○--, f; --△--, θ.

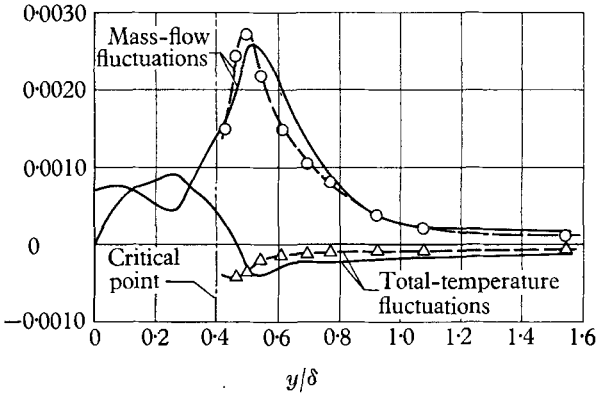

FIGURE 12. Mass-flow and total-temperature distributions for neutral oscillation, $M_e = 2{\cdot}2$. ——, Present theory, $Re_\theta = 535$, $c = 0{\cdot}616$. Laufer–Vrebalovich data, $Re_\theta = 400$, $c = 0{\cdot}62$: --○--, mass-flow fluctuations; --△--, total-temperature fluctuations.

quite as good. Laufer (1959) indicates that in locally subsonic and transonic flows there is some doubt involved in deducing pressure, velocity, and temperature fluctuation amplitudes from the mean-square hot-wire output. At local Mach numbers above 1·2, the calibration of hot wires is well standarized (Laufer & McClellan 1955), but such is not the case at transonic speeds. In addition, Laufer & Vrebalovich had to assume the values of pressure fluctuation amplitude in order to deduce velocity and temperature fluctuation amplitudes. The question

of assumed pressure-fluctuation level is removed when the mass-flow and total-temperature fluctuations from theory and experiment are compared. This comparison is shown in figure 12, and the agreement here is quite good.

4.2.2. *Mach number* 5·6. The situation at Mach number 5·6 is quite different from that described for Mach number 2·2. The dominant factor here is the behaviour of the imaginary part of the inviscid solution $-w'_w G_{i_w}/c$, which is proportional to $(w'/T)'_c|\pi_c/\pi_w|^2$. At $M_e = 5{\cdot}6$, this quantity is also slightly dependent on α, but in figure 13 it will be considered as dependent only on c and independent of α. Because at $M_e = 5{\cdot}6$, $|\pi_c/\pi_w|^2 \ll 1$ (figure 7), the quantity $-w'_w G_{i_w}/c$ is very small in magnitude, so small that the viscous solutions to the scale of the sketch

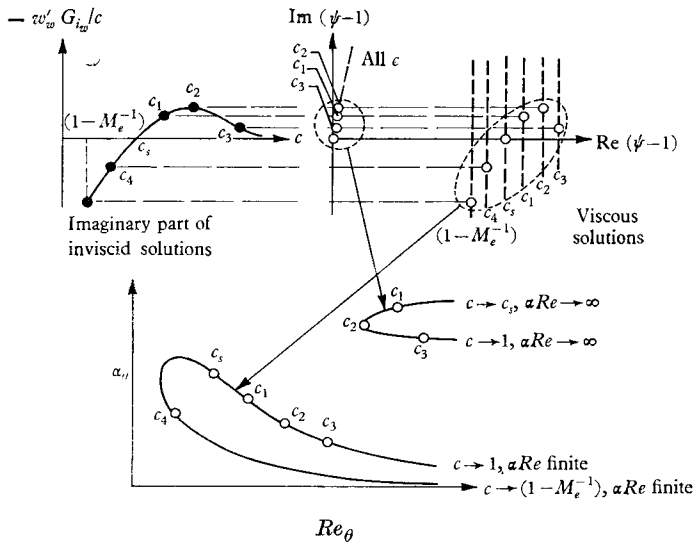

FIGURE 13. Schematic construction of neutral stability diagram at $M_e = 5{\cdot}6$.

are just vertical lines. The value of this quantity is no longer monotonic in c. Rather it increases with c to a maximum at some value of $c > c_s$ and then decreases toward zero as $c \to 1$.

The construction of the neutral stability diagram is as follows. For $c = c_s$, there are two solutions, one of which is that of the neutral inviscid oscillation. As c increases toward unity, two solutions are continually obtained. There is no longer the phenomenon of a maximum value of c above which no neutral oscillations can occur. This behaviour occurs because the maximum value of $-w'_w G_{i_w}/c$ from the inviscid solutions (occurring for $c = c_2$ in figure 13) is much less than the maximum value of $\mathrm{Im}(\psi - 1)$ at the pertinent value of c. For $[1 - (1/M_e)] < c < c_s$ there is only one intersection. The solutions for neutral oscillations form two loops in figure 13.

The two loops obtained at Mach number 5·6 are shown in figure 14. The upper right loop has a minimum Reynolds number based on momentum thickness of slightly over 10^5. This value of Re_θ corresponds to a length Reynolds number greater than 10^{10}, and it is not likely that this loop has much practical significance.

The data obtained by Demetriades (1958, 1960) at Mach number 5·8 are identified with the curve in the lower left corner of figure 14. The portions of this curve drawn in a full unbroken line have about the same shape as Demetriades's data, but are about an order of magnitude lower in Reynolds number than the experimental data. Nevertheless, as shown in figure 14, a selected point on the curve is about an order of magnitude higher in Reynolds number than obtained using the Lees–Lin and Dunn–Lin theories. This behaviour shows the importance of the new dissipation and shear terms presently included. The value of $\bar{\epsilon}$ for this test point is 2·0, showing that there is no reason to expect good quantitative agreement between theory and experiment.

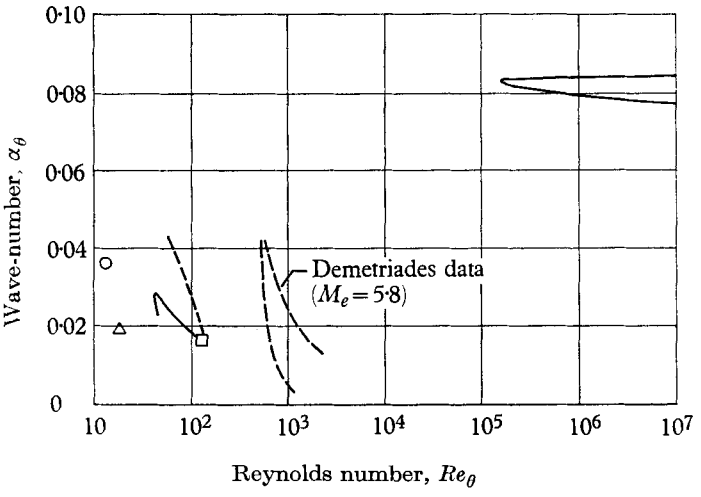

FIGURE 14. Neutral stability characteristics, $M_e = 5{\cdot}6$. For point at $\eta_c = 17{\cdot}4$, $c = 0{\cdot}98099$: □, present calculations; Δ, Dunn–Lin viscous solution; ○, Lees–Lin viscous solution.

The dashed portion of the lower loop is that portion where the propagation velocity c very closely approaches unity. It is suspected that the calculation procedure is inadequate for this portion of the curve, since the splitting of the solutions into inviscid and viscous types is of questionable validity for $c \to 1$. It can be shown that a necessary condition for splitting the solutions into inviscid and viscous types is that $[\alpha Re(1-c)] \gg \alpha^2$.

4.2.3. *Discussion.* From the results obtained thus far, it is of some interest to compare the neutral stability behaviour of insulated boundary layers over a wide range of Mach numbers. Because these comparisons are based on only a few calculated stability diagrams, some of which are not well understood, parts of the discussion that follows must be considered speculative.

For Mach numbers of 2·2 and below, only a single stability loop is obtained both theoretically and experimentally (Laufer & Vrebalovich 1958, 1960; Schubauer & Skramstad 1948). At Mach number 5·6, two loops are obtained, neither of which is related to the one obtained at $M_e \leqslant 2{\cdot}2$. We may perhaps describe the stability behaviour from Mach number zero to about Mach number 2·5

as 'almost incompressible';† that above about Mach number 5 as 'hypersonic'; this leaves a very interesting and little understood transition region from one type of stability behaviour to the other between Mach numbers of about 2·5 and 5. Some numerical results were obtained for the 'transitional' case $M_e = 3{\cdot}2$, but these results are not well enough understood to be discussed here.

The variation of minimum critical Reynolds number with Mach number is also quite interesting. The calculated value of $(Re_\theta)_{\min\,\mathrm{crit}}$ decreases from a value of about 150 at Mach number zero (Lees 1947), through a value of about 45 at Mach number 2·2, to some value below 10 at Mach number 3·2. All these values are obtained from the conventional 'almost incompressible' loop. At Mach number 5·6, the calculated value of $(Re_\theta)_{\min\,\mathrm{crit}}$ is about 45 (figure 8) and comes from the new lower loop. These results indicate that the minimum critical Reynolds number decreases from its Mach-number-zero value, reaches a minimum somewhere around Mach number 3 and then increases again.

One may speculate about the variation of minimum critical Reynolds number at hypersonic speeds. For the lowest loop, the calculated values of $\alpha_\theta Re_\theta$ are about the same for both $M_e = 3{\cdot}2$ and $M_e = 5{\cdot}6$. If $\alpha_\theta Re_\theta$ remains fairly constant hypersonically and α_θ follows the asymptotic trend, $\alpha_\theta \sim (1/M_e^2)$ (figure 2), then $(Re_\theta)_{\min\,\mathrm{crit}}$ would increase as M_e^2 [and $(Re_x)_{\min\,\mathrm{crit}}$ as M_e^4]. We can infer that instability of the laminar boundary layer would move downstream very rapidly with increase in local Mach number. There is some experimental evidence supporting this latter speculation, namely, that Bogdonoff (1959) reports that he has never observed transition to occur at a local Mach number of 11 even at length Reynolds numbers as high as 10^7.

5. Qualitative description of compressible-boundary-layer stability

The examples of the previous section (§ 4) show that the theoretical and experimental neutral stability characteristics and amplitude distributions are in at least qualitative agreement. For a better understanding of the stability phenomenon it is useful to discuss the balance of disturbance energy,

$$\begin{bmatrix}\text{Net energy}\\ \text{change per}\\ \text{cycle}\end{bmatrix} = \begin{bmatrix}\text{Net 'production' of}\\ \text{disturbance energy}\\ \text{per cycle}\end{bmatrix} - \begin{bmatrix}\text{Dissipation}\\ \text{per cycle}\end{bmatrix}. \tag{105}$$

For a neutral disturbance the net energy change per cycle is zero. By 'production' in equation (105) is meant the transfer of energy from the mean flow to the disturbance flow. The net production term is expressed in terms of the Reynolds stress:

$$\begin{bmatrix}\text{Net production of}\\ \text{disturbance energy}\\ \text{per cycle}\end{bmatrix} = \int_0^\lambda \int_0^\infty \tau \frac{\partial u}{\partial y}\, dy\, dx, \tag{106}$$

† Laufer & Vrebalovich (1960) have in fact recently correlated the experimental results of Schubauer & Skramstad (1948) for incompressible flow and those of Laufer & Vrebalovich (1960) at $M_e = 1{\cdot}6$ and $M_e = 2{\cdot}2$. By plotting $(\beta\nu_e/u_e^2)$ against Re_δ, where δ is the full boundary-layer thickness, they obtain a single diagram for all three Mach numbers. The amplification factors plotted as $(\alpha c_i \delta)/u_e$ against $(\beta\nu_e/u_e^2)$ also correlate for these experiments. These observations support the identification of the neutral stability characteristics at Mach numbers up to about 2·5 as almost incompressible.

where $$\tau = -\rho\overline{u'v'} = -\tfrac{1}{2}\alpha\rho\mathrm{Re}(f\phi^*).\dagger \tag{107}$$

Some knowledge of the behaviour of the Reynolds stress (therefore also the velocity fluctuation amplitudes) will prove desirable in understanding the effects of compressibility.

For a real gas, the longitudinal velocity and temperature fluctuations must vanish at the wall no matter how small the viscosity and thermal conductivity. Thus, we must add viscous solutions that take on the wall values $-(f_{\mathrm{inv}})_w$ and $-(\theta_{\mathrm{inv}})_w$ to the inviscid functions already determined (figure 1). An approximate form of these viscous solutions is obtained by considering the asymptotic form of the viscous equations (41) to (43). In a thin layer near the wall ($w \approx 0$), equations (41) to (43) become

$$f_v''' + (i\alpha Rec/\nu_w)f_v' = 0, \tag{108}$$

$$\phi_v' = -if_v - (ic/T_w)\theta_v, \tag{109}$$

$$\theta_v'' + (i\alpha Re\sigma c/\nu_w)\theta_v = 0. \tag{110}$$

The desired solutions to equations (108) and (110) are those which decay to zero far from the wall; they are, respectively,

$$f_v = -(f_{\mathrm{inv}})_w \exp\{-(1-i)\,y/\delta_w\}, \tag{111}$$

$$\theta_v = -(\theta_{\mathrm{inv}})_w \exp\{-(1-i)\,y\sigma^{\frac{1}{2}}/\delta_w\}, \tag{112}$$

where $\delta_w = (2\nu_w/c\alpha Re)^{\frac{1}{2}}$ is representative of the thickness of the layer near the wall in which the viscosity effects are important.

According to the continuity equation (109), a viscous normal-velocity fluctuation is induced by f_v and θ_v. Since $\phi_v(\infty) = 0$, by utilizing equations (111) and (112) in equation (109), one obtains

$$\int_\infty^0 \phi_v' dy = (\phi_v)_w - \phi_v(\infty) = (\phi_v)_w = -\tfrac{1}{2}i(1+i)\,\delta_w(f_{\mathrm{inv}})_w(1+\tilde{K}\sigma^{-\frac{1}{2}}), \tag{113}$$

where $$\tilde{K} \equiv (\gamma-1)M_e^2c^2/T_w. \tag{114}$$

But $\phi_w = (\phi_v)_w + (\phi_{\mathrm{inv}})_w = 0$, so that $(\phi_{\mathrm{inv}})_w = -(\phi_v)_w$, and the inviscid solutions must now be altered slightly to satisfy the boundary condition at the wall.

In the case of a fictitious inviscid gas, the Reynolds stress for a neutral disturbance must vanish everywhere. But for the real gas $(\phi_{\mathrm{inv}})_w \neq 0$, and the Reynolds stress associated with the inviscid solutions is [equations (107), (113), and (114)]

$$\tau_{\mathrm{inv}}(\delta_w) = \tfrac{1}{4}\rho_w\alpha\delta_w|(f_{\mathrm{inv}})_w|^2(1+\tilde{K}\sigma^{-\frac{1}{2}}). \tag{115}$$

[Note that $\tau_{\mathrm{inv}}(\delta_w) > 0$ and is of order $Re^{-\frac{1}{2}}$.] Now, since the Reynolds stress for the inviscid solution is constant in any region where the Wronskian of the two solutions π_r and π_i (or ϕ_r and ϕ_i) is continuous (Lees & Lin 1946), this Reynolds stress must be constant in the region between the wall and the critical layer, as shown by the broken line in figure 15. But $\tau \to 0$ far from the wall, so the value of τ given by equation (115) must be cancelled by an equal and opposite increment in Reynolds stress at the critical layer. This incremental jump in Reynolds stress

† Of course the 'mean flow' is also altered slightly by the action of the Reynolds stress (Stuart 1956), but this effect is of order a^2Re, where a is here the disturbance amplitude, and makes a second-order correction to the disturbance flow.

in the neighbourhood of the critical layer is a viscous phenomenon. However, its value can be calculated from the inviscid solutions, and viscosity has the effect of smoothing the transition from one value to the other. This behaviour is analogous to the one-dimensional normal shock wave, which is a viscous conductive phenomenon whose gross characteristics can be determined without considering viscosity and conductivity, but whose detailed structure can only be determined through consideration of the effects of viscosity and thermal conductivity.

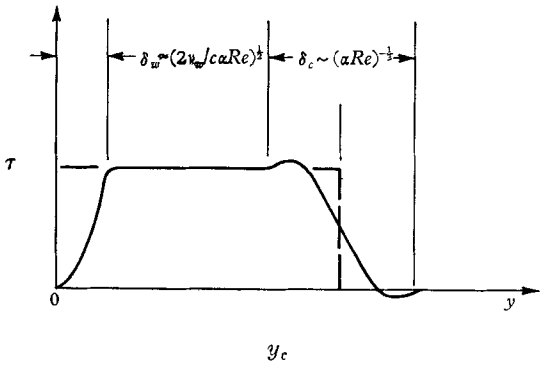

FIGURE 15. Sketch of Reynolds stress distribution for $\alpha Re \gg 1$, $(c > c_s)$.

The magnitude of the jump in Reynolds stress from equations (76) to (79) and (107) is

$$[\tau]_{y_c-0}^{y_c+0} = -\frac{\alpha}{2}\frac{c}{T_w w_w'}|(f_{\text{inv}})_w|^2 v_0(c)\left|\frac{\pi_c}{\pi_w}\right|^2, \tag{116}$$

where

$$v_0(c) \equiv -\pi\frac{w_w'}{T_w}\frac{cT_c^2}{w_c'^3}\left[\frac{d}{dy}\left(\frac{w'}{T}\right)\right]_c. \tag{117}$$

This function arises continually in hydrodynamic stability problems (Lin 1955) and is in fact included in the compressible-boundary-layer tabulations of Mack (1958). Along the upper branch $c > c_s$, $A < 0$, $v_0(c) > 0$ so that the jump in Reynolds stress is negative as required. Setting the sum of equations (115) and (116) equal to zero and remembering that $\delta_w = (2\nu_w/\alpha Rec)^{\frac{1}{2}}$ yields

$$(\alpha Re)^{\frac{1}{2}} = \left(\frac{\nu_w w_w'^2}{2c^3}\right)^{\frac{1}{2}}\frac{(1+\tilde{K}\sigma^{-\frac{1}{2}})}{v_0(c)\,|\pi_c/\pi_w|^2}. \tag{118}$$

This expression is strictly valid only for $\alpha Re \gg 1$, and its significance is that as the Mach number increases, $\tilde{K}$ increases [from equation (114)] while $|\pi_c/\pi_w|^2$ decreases (see figure 7). Both of these effects tend to extend the upper neutral boundary to larger values of αRe, and are to be interpreted as destabilizing since they enlarge the region of amplified disturbances.

The sharp decrease in $|\pi_c/\pi_w|$ shown in figure 7 occurs when the wall is supersonic with respect to the wave. This behaviour can be ascertained from an approximate analysis of the inviscid equation. Near the wall, $\phi \approx 0$, so that $\pi' \approx 0$ and equation (16) may be written

$$\pi'' + \alpha^2[(M_{\text{rel}})_w^2 - 1]\pi = 0, \tag{119}$$

where

$$(M_{\text{rel}})_w = M_e c/T_w^{\frac{1}{2}}. \tag{120}$$

Equation (119) is just the Prandtl–Glauert equation for a wavy disturbance in a steady flow. Through a Dorodnitsyn–Howarth transformation $\tilde{\eta} = \int \frac{dy}{T}$, the boundary-layer thickness is normalized and equation (119) becomes

$$d^2\pi/d\tilde{\eta}^2 + (\alpha T_w)^2 [(M_{\mathrm{rel}})_w^2 - 1]\pi = 0. \tag{121}$$

At subsonic or slightly supersonic free-stream speeds, $(\alpha T_w)^2 = O(\alpha^2)$ and the *increase* in pressure amplitude between the plate surface and the critical layer is small. But at high supersonic and hypersonic speeds, $(\alpha T_w)^2$ is no longer small and $(M_{\mathrm{rel}})_w > 1$, so that the *decrease* in pressure fluctuation amplitude outward to the critical layer is substantial. This phenomenon was not properly accounted for in previous theoretical treatments (Lees & Lin 1946; Dunn & Lin 1955) because the inviscid solutions were obtained by employing series expansions in powers of α^2. Since α^2 was supposed to be small, it was tacitly assumed that $|\pi_c/\pi_w|^2 = O(1)$. The fact that $|\pi_c/\pi_w|^2 \ll 1$ for high Mach number flows has a strong influence on the Reynolds stress increment at the critical layer [equation (116)] and therefore on the energy balance for a neutral disturbance.

For neutral disturbances at very large values of αRe, the Reynolds stress has the distribution through the boundary layer shown by the solid line in figure 15.

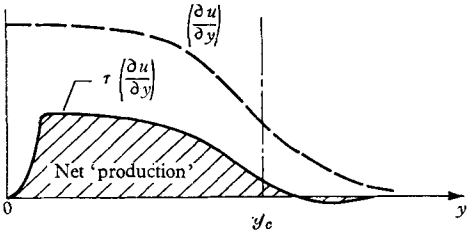

FIGURE 16. Net conversion of energy from mean flow to disturbance flow.

The net production of energy may also be sketched (figure 16). The shaded area, being the integral under the $\tau(\partial u/\partial y)$ curve, represents the net energy production per cycle. It is this quantity that must be balanced by dissipation for a neutral oscillation.

For αRe only moderately large, the two regions in the boundary layer where viscosity is important tend to grow and may even overlap, so that a region of constant Reynolds stress may not be observed between the wall and the critical layer. As an example of the Reynolds stress distribution for moderately large αRe, that corresponding to the amplitude distributions of figures 11 and 12 is shown in figure 17. The broken line in figure 17 is the level of the inviscid Reynolds stress between the wall and the critical layer. When $c < c_s$, the overlapping of the two viscous regions must always occur because the jump in Reynolds stress predicted by the inviscid solutions across the critical layer [equation (116)] is positive and can never counterbalance the Reynolds stress produced near the wall.

Even when αRe is not large, the following qualitative effects remain: the production of disturbance energy at the wall increases with Mach number; the stabilizing or destabilizing effect at the critical layer diminishes in the ratio

$|\pi_c/\pi_w|^2$, and at high Mach number may be of negligible importance. Both of these tendencies indicate that, as the Mach number increases, the net production of disturbance energy also increases, so that the dissipation effects must become more important. As indicated by the calculations at Mach number 5·6, this behaviour significantly lowers the range of αRe for neutral disturbances to a level such that Prandtl's splitting of the disturbance flow into inviscid and viscous parts is no longer appropriate for a proper quantitative estimation of the stability characteristics of a given boundary-layer profile.

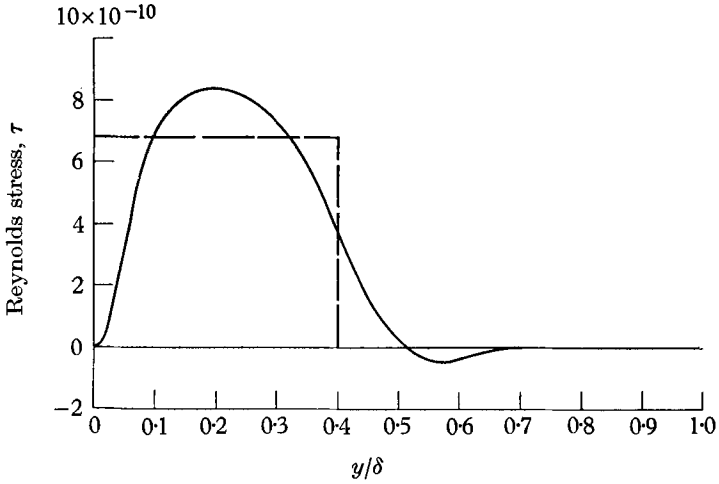

FIGURE 17. Reynolds stress distribution for neutral oscillation, $M_e = 2{\cdot}2$, $c = 0{\cdot}616$, $Re_\theta = 535$: — — —, inviscid solution; ——, complete solution.

6. Concluding remarks

The present study of the stability of the compressible laminar boundary layer shows that, although the basic stability mechanisms are the same as for incompressible flow, the relative importance of the various mechanisms changes considerably with Mach number.

1. Instead of being nearly constant across the boundary layer, the amplitude of inviscid pressure fluctuations decreases markedly with distance from the plate surface at Mach numbers greater than 3. Because of this behaviour the rate of absorption (or production) of disturbance energy near the critical layer is greatly reduced, as compared with subsonic or slightly supersonic flows.

2. At the same time the rate of production of disturbance energy near the surface caused by the viscous phase-shifts increases with Mach number.

3. Viscous dissipation becomes extremely important at high Mach number, since it must compensate for the effects mentioned in items 1 and 2. This phenomenon is also foreshadowed by the increase in the relative magnitude of the temperature fluctuations. Accordingly, terms in the equations of motion involving gradients of viscosity or conductivity fluctuation, or viscous dissipation, which are neglected in the older analyses, must be included at high Mach numbers.

4. For free-stream Mach numbers of 2·2 and below, only a single stability loop

in the (α, Re)-diagram is obtained. Calculated neutral-stability characteristics and disturbance-amplitude distributions at $M_e = 2{\cdot}2$ are in good agreement with the Laufer–Vrebalovich data.

5. At $M_e = 5{\cdot}6$ two distinct stability loops are obtained, but the minimum Reynolds number (Re_θ) for the upper loop is so high ($\sim 10^5$) that it does not have much practical significance. The other loop is qualitatively similar to the experimental results of Demetriades at $M_e = 5{\cdot}8$. However, the calculated Reynolds numbers are still an order of magnitude lower than the experimental values, although they are in turn an order of magnitude larger than the values obtained from the Lees–Lin or Dunn–Lin methods.

6. At Mach numbers around 3·5, one obtains a transitional stability diagram between the 'almost incompressible' behaviour for $M_e \leqslant 2{\cdot}5$ and the hypersonic behaviour for $M_e \geqslant 5{\cdot}0$. This regime requires additional theoretical study.

7. The structure and solutions of the linearized disturbance equations must be carefully examined for the case $c_r \to 1$. In addition there is some question concerning the uniqueness of the wave-number eigenvalues for a neutral inviscid disturbance when the relative velocity between the wave and the plate surface is supersonic.

8. Asymptotic methods utilized in all boundary-layer-stability analyses, based on a 'small' parameter of the form $\epsilon = (\alpha Re)^{-\frac{1}{2}}$, are no longer adequate at high Mach numbers. In fact, the procedure of splitting the solutions into 'viscous' (rapidly varying) and inviscid (slowly varying) is no longer justified. It is suggested that attempts be made to integrate the complete, linearized disturbance equations, perhaps by methods similar to those developed in the present study for the separate viscous and inviscid solutions.

9. Some evidence exists that αRe at first decreases with increasing Mach number, and then approaches a constant value as viscous dissipation builds up. Since the wave-number behaves asymptotically like $1/M_e^2$, the minimum critical Reynolds number is likely to increase sharply for hypersonic speeds.

This paper is taken from the thesis submitted by the junior author to The California Institute of Technology in partial fulfilment of the requirements for the degree of Doctor of Philosophy. For a more detailed development of many of the items presented herein, the reader is referred to the thesis itself, Reshotko (1960). A short account of some of the main theoretical problems and physical mechanisms of laminar boundary-layer stability at high Mach numbers is given in Lees & Reshotko (1960).

The authors wish to acknowledge many helpful discussions with Dr John Laufer and Dr Leslie M. Mack of the Jet Propulsion Laboratory and to thank Mr Kenneth Lock for programing and performing all high-speed digital computer calculations. The authors also acknowledge the sponsorship and financial support of the Office, Chief of Ordnance, Office of Ordnance Research, and Army Ballistic Missile Agency, Contract No. DA-04-495-Ord-19. The junior author gratefully acknowledges the receipt of a Daniel and Florence Guggenheim Fellowship in Jet Propulsion for the academic years 1957–59 and partial support from the Out-Service Training Program of the NASA.

REFERENCES

BOGDONOFF, S. M. 1959 Private communication.

CHENG, S. I. 1953 On the stability of laminar boundary-layer flow. *Princeton Univ. Aero. Engng Lab. Rep.* no. 211. Also, *Quart. Appl. Math.* **11**, 346–50.

DEMETRIADES, A. 1958 An experimental investigation of the stability of the hypersonic laminar boundary layer. *GALCIT Hypersonic Res. Project, Memo.* no. 43.

DEMETRIADES, A. 1960 An experiment on the stability of the hypersonic laminar boundary layer. *J. Fluid Mech.* **7**, 385.

DUNN, D. W. 1953. On the stability of the laminar boundary layer in a compressible fluid. *Thesis, Mass. Inst. Tech.*

DUNN, D. W. & LIN, C. C. 1955 On the stability of the laminar boundary layer in a compressible fluid. *J. Aero. Sci.* **22**, 455–77.

HOLSTEIN, H. 1950 Über die aussere und innere Reibungsschicht bei Störungen laminarer Strömungen. *Z. angew. Math. Mech.* **30**, 25–49.

LAUFER, J. 1959 Private communication.

LAUFER, J. & MCCLELLAN, R. 1955 Measurements of heat transfer from fine wires in supersonic flow. *Jet Prop. Lab. Cal. Inst. Tech. Ext. Publ.* no. 315.

LAUFER, J. & VREBALOVICH, T. 1958 Stability of a supersonic laminar boundary layer on a flat plate. *Jet Prop. Lab. Cal. Inst. Tech. Rep.* no. 20–116.

LAUFER, J. & VREBALOVICH, T. 1960 Stability and transition of a supersonic laminar boundary layer on an insulated flat plate. *J. Fluid Mech.* **9**, 257–99.

LEES, L. 1947 The stability of the laminar boundary layer in a compressible fluid. *NACA Rep.* no. 876.

LEES, L. & LIN, C. C. 1946 Investigation of the stability of the laminar boundary layer in a compressible fluid. *NACA TN* no. 1115.

LEES, L. & RESHOTKO, E. 1960 Stability of the compressible laminar boundary layer. *AGARD, NATO, Rep.* no. 268.

LIGHTHILL, M. J. 1950 Reflection at a laminar boundary layer of a weak steady disturbance to a supersonic stream neglecting viscosity and heat conduction. *Quart. J. Mech. Appl. Math.* **3**, 303–25.

LIN, C. C. 1955 *The Theory of Hydrodynamic Stability.* Cambridge University Press.

MACK, L. M. 1958 Calculation of the laminar boundary layer on an insulated flat plate by the Klunker-McLean method. *Jet Prop. Lab. Cal. Inst. Tech. Prog. Rep.* no. 20–352.

MACK, L. M. 1960 Numerical calculation of the stability of the compressible laminar boundary layer. *Jet Prop. Lab. Cal. Inst. Tech. Rep.* no. 20–122.

MILES, J. W. 1959 On panel flutter in the presence of a boundary layer. *J. Aero/Sp. Sci.* **26**, 81–93.

PRANDTL, L. 1935 *The mechanics of viscous fluids.* Article in Durand, W. R. (ed.), *Aerodynamic Theory*, Vol. III, Div. G. Berlin: Julius Springer.

RESHOTKO, E. 1960 Stability of the compressible laminar boundary layer. *Cal. Inst. Tech. Ph.D. Thesis.* Also *GALCIT Hypersonic Res. Project, Memo.* no. 52.

SCHLICHTING, H. 1935 Amplitudenverteilung und Energiebilanz der kleinen Störungen bei der Plattengrenzschicht. *Nachr. Ges. Wiss. Göttingen, Math-Phys. Klasse*, **1**, 47–9. (Translated as *NACA TM* no. 1265, 1950.)

SCHUBAUER, G. B. & SKRAMSTAD, H. K. 1948 Laminar boundary-layer oscillations and transition on a flat plate. *NACA Rep.* no. 909.

STUART, J. T. 1956 On the effects of the Reynolds stress on hydrodynamic stability. *Z. angew. Math. Mech. Sonderheft*, 532–38.

TOLLMIEN, W. 1947 Asymptotische Integration der Störungsdifferential-gleichung ebener laminarer Strömungen bei hohen Reynoldsschen Zahlen. *Z. angew. Math. Mech.* **25/27**, 33–50; 70–83.

VAN DRIEST, E. R. 1952 Calculation of the stability of the laminar boundary layer in a compressible fluid on a flat plate with heat transfer. *J. Aero. Sci.* **19**, 801–12.

Symbols

The symbols used in the present report are in general those commonly used in the literature on boundary-layer stability.

	Dimensional quantities	Dimensionless quantities	Reference quantities
Positional co-ordinates:			
Longitudinal	x^*	x	$(\nu_e^* x^*/u_e^*)^{\frac{1}{2}}$
Normal	y^*	y	$(\nu_e^* x^*/u_e^*)^{\frac{1}{2}}$
Time	t^*	t	$(\nu_e^* x^*/u_e^{*3})^{\frac{1}{2}}$
Velocity components:			
Longitudinal	$u^* = \bar{u}^* + u^{*\prime}$	$w(y) + f(y)\, e^{i\alpha(x-ct)}$	u_e^*
Normal	$v^* = \bar{v}^* + v^{*\prime}$	$v(y) + \alpha\phi(y)\, e^{i\alpha(x-ct)}$	u_e^*
Density	$\rho^* = \bar{\rho}^* + \rho^{*\prime}$	$\rho(y) + r(y)\, e^{i\alpha(x-ct)}$	ρ_e^*
Pressure	$p^* = \bar{p}^* + p^{*\prime}$	$p(y) + \pi(y)\, e^{i\alpha(x-ct)}$	p_e^*
Temperature	$T^* = \bar{T}^* + T^{*\prime}$	$T(y) + \theta(y)\, e^{i\alpha(x-ct)}$	T_e^*
Viscosity coefficients	$\mu^* = \bar{\mu}^* + \mu^{*\prime}$	$\mu(y) + m(y)\, e^{i\alpha(x-ct)}$	μ_e^*
	$\mu_2^* = \bar{\mu}_2^* + \mu_2^{*\prime}$	$\mu_2(y) + m_2(y)\, e^{i\alpha(x-ct)}$	μ_e^*
Thermal conductivity	$k^* = \bar{k}^* + k^{*\prime}$	$\sigma^{-1}\mu(y) + \sigma^{-1}m(y)\, e^{i\alpha(x-ct)}$	$c_p\mu_e^*$
Wavelength	λ^*	λ	$(\nu_e^* x^*/u_e^*)^{\frac{1}{2}}$
Wave-number	$\alpha^* = 2\pi/\lambda^*$	$\alpha = 2\pi/\lambda$	$(u_e^*/\nu_e^* x^*)$
Disturbance propagation velocity	c^*	c	u_e^*

M_e	Local Mach number outside mean boundary layer
R^*	Gas constant
Re	Reynolds number based on reference length
Re_x	Length Reynolds number
Re_θ	Reynolds number based on momentum thickness
T_0	Stagnation temperature of external stream
α_θ	Momentum-thickness wave-number, $2\pi\theta/\lambda$
γ	Ratio of specific heats
δ	Boundary-layer thickness
δ_c	Thickness of viscous layer about critical point, of order $(\alpha Re)^{-\frac{1}{3}}$
δ_w	Thickness of viscous layer near wall
ϵ	Small parameter; $(\alpha Re)^{-\frac{1}{3}}$ for Lees–Lin ordering, $(\alpha Re)^{-\frac{1}{4}}$ for Dunn–Lin ordering
$\bar{\epsilon}$	Small parameter; $(\alpha Re_{\text{ref}})^{-\frac{1}{3}}$ for present ordering
ν	Kinematic viscosity
σ	Prandtl number
τ	Reynolds stress

Subscripts

c	Quantity evaluated at critical point
corr	Inviscid function corrected for viscous effects about critical layer
e	Local condition outside mean boundary layer (external)
inv	Inviscid
o	Outer condition
s	Quantity for neutral inviscid disturbance
v	Viscous
w	Quantity evaluated at wall

A bar over a quantity indicates mean value.

Primes generally denote differentiation with respect to y. The few instances where primes denote a fluctuating quantity should not cause any confusion.